AD-A193 188 ENVIRONMENTAL IMPACT RESEARCH PROGRAM: COUPLING HYDRODYNAMICS TO A MULTIP..(U) ARMY ENGINEER WATERWAYS EXPERIMENT STATION VICKSBURG MS ENVIR.. 1/1

UNCLASSIFIED S L BIRD ET AL. MAR 88 WES/TR/EL-88-7 F/G 24/4 NL

END
DATE
FILMED
7 88

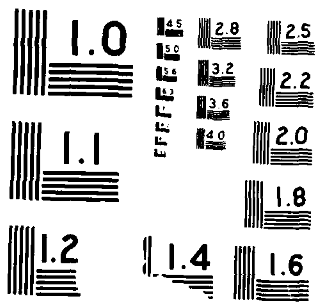
1.0
4.5
5.0
5.6
2.8
3.2
3.6
4.0
2.5
2.2
2.0
1.1
1.8
1.2
1.4
1.6

US Army Corps of Engineers

AD-A193 188

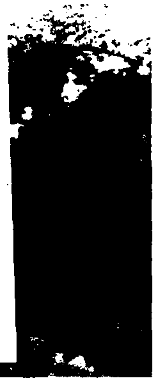

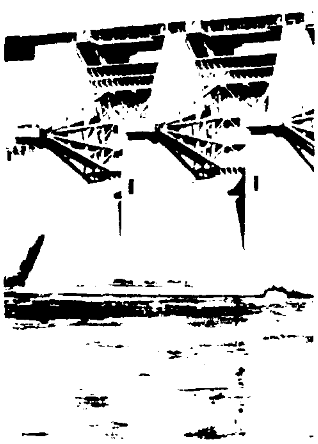

(4)

DTIC FILE COPY

ENVIRONMENTAL IMPACT RESEARCH PROGRAM

TECHNICAL REPORT EL-88-7

COUPLING HYDRODYNAMICS TO A MULTIPLE-BOX WATER QUALITY MODEL

by

Sandra L. Bird, Ross Hall

Environmental Laboratory

DEPARTMENT OF THE ARMY
Waterways Experiment Station, Corps of Engineers
PO Box 631, Vicksburg, Mississippi 39180-0631

March 1988
Final Report

88-5-05 020

Prepared for DEPARTMENT OF THE ARMY
US Army Corps of Engineers
Washington, DC 20314-1000

Under EIRP Work Unit No. 31730

88 5 05 020

Destroy this report when [illegible]
it to the [illegible]

[illegible]

Unclassified
SECURITY CLASSIFICATION OF THIS PAGE

REPORT DOCUMENTATION PAGE

Form Approved
OMB No. 0704-0188

1a. REPORT SECURITY CLASSIFICATION
Unclassified

1b. RESTRICTIVE MARKINGS

2a. SECURITY CLASSIFICATION AUTHORITY

2b. DECLASSIFICATION / DOWNGRADING SCHEDULE

3. DISTRIBUTION / AVAILABILITY OF REPORT
Approved for public release; distribution unlimited.

4. PERFORMING ORGANIZATION REPORT NUMBER(S)
Technical Report EL-88-7

5. MONITORING ORGANIZATION REPORT NUMBER(S)

6a. NAME OF PERFORMING ORGANIZATION
USAEWES
Environmental Laboratory

6b. OFFICE SYMBOL (If applicable)

7a. NAME OF MONITORING ORGANIZATION

6c. ADDRESS (City, State, and ZIP Code)
PO Box 631
Vicksburg, MS 39180-0631

7b. ADDRESS (City, State, and ZIP Code)

8a. NAME OF FUNDING/SPONSORING ORGANIZATION
US Army Corps of Engineers

8b. OFFICE SYMBOL (If applicable)

9. PROCUREMENT INSTRUMENT IDENTIFICATION NUMBER

8c. ADDRESS (City, State, and ZIP Code)
Washington, DC 20314-1000

10. SOURCE OF FUNDING NUMBERS

PROGRAM ELEMENT NO.	PROJECT NO.	TASK NO.	WORK UNIT ACCESSION NO.
			31730

11. TITLE (Include Security Classification)
Coupling Hydrodynamics to a Multiple-Box Water Quality Model

12. PERSONAL AUTHOR(S)
Bird, Sandra L.; Hall, Ross

13a. TYPE OF REPORT
Final report

13b. TIME COVERED
FROM ______ TO ______

14. DATE OF REPORT (Year, Month, Day)
March 1988

15. PAGE COUNT
53

16. SUPPLEMENTARY NOTATION
Available from National Technical Information Service, 5285 Port Royal Road, Springfield, VA 22161.

17. COSATI CODES

FIELD	GROUP	SUB-GROUP

18. SUBJECT TERMS (Continue on reverse if necessary and identify by block number)
DeGray Lake
Mississippi Sound
Numerical models
Savannah River Estuary
Water quality
Water Quality Analysis Simulation Program

19. ABSTRACT (Continue on reverse if necessary and identify by block number)

Long-term, multidimensional water quality modeling, using directly linked hydrodynamic and water quality models, can become prohibitively expensive. In this report, fine scale, short time-step hydrodynamic model output is linked with coarse grid, longer time-step multiple-box water quality model. The formulation, limitations, and adaption for use in applications of the Water Quality Analysis Simulation Program (WASP), the US Environmental Protection Agency multiple-box model, are discussed. Linkage of the multiple-box model to two hydrodynamic models is explained. Dye tracer simulations are used to compare mass transport by the box model with mass transport by the directly linked models for three applications: Savannah River Estuary, Mississippi Sound, and DeGray Lake.

20. DISTRIBUTION / AVAILABILITY OF ABSTRACT
☒ UNCLASSIFIED/UNLIMITED ☐ SAME AS RPT ☐ DTIC USERS

21. ABSTRACT SECURITY CLASSIFICATION
Unclassified

22a. NAME OF RESPONSIBLE INDIVIDUAL

22b. TELEPHONE (Include Area Code)

22c. OFFICE SYMBOL

DD Form 1473, JUN 86 Previous editions are obsolete.

SECURITY CLASSIFICATION OF THIS PAGE
Unclassified

SECURITY CLASSIFICATION OF THIS PAGE

SECURITY CLASSIFICATION OF THIS PAGE

PREFACE

This report was prepared by the Environmental Laboratory (EL) of the US Army Engineer Waterways Experiment Station (WES), as part of the Environmental Impact Research Program (EIRP), Work Unit No. 31730, "Environmental Impacts of Modifying Estuarine Circulation and Transport Processes." The EIRP is sponsored by the Office, Chief of Engineers (OCE), US Army, Washington, DC. The OCE Technical Monitors for EIRP are Dr. John Bushman and Dr. David Buelow. Mr. Dave Mathis is the Water Resources Support Center Technical Monitor.

This report describes the use of a box-type model for transport/water quality calculations and the linkage of this model to multidimensional hydrodynamic models. Performance of the coarser grid/time-step box model is compared with directly linked transport codes.

The study was conducted and the report was prepared by Ms. Sandra L. Bird and Mr. Ross Hall of the Water Quality Modeling Group (WQMG), Ecosystem Research and Simulation Division (ERSD), EL, under the direct supervision of Mr. Mark Dortch, Chief, WQMG. General supervision was provided by Mr. Donald L. Robey, Chief, ERSD, and Dr. John Harrison, Chief, EL. Dr. Roger T. Saucier was Program Manager of EIRP. The report was edited by Ms. Lee T. Byrne of the Information Products Division, Information Technology Laboratory.

Commander and Director of WES during the preparation and publication of this report was COL Dwayne G. Lee, CE. Dr. Robert W. Whalin was the Technical Director.

This report should be cited as follows:

Bird, Sandra L., and Hall, Ross. 1988. "Coupling Hydrodynamics to a Multiple-Box Water Quality Model," Technical Report EL-88-7, US Army Engineer Waterways Experiment Station, Vicksburg, Miss.

CONTENTS

CONVERSION FACTORS, NON-SI TO SI (METRIC)
UNITS OF MEASUREMENT

Non-SI units of measurement used in this report can be converted to SI (metric) units as follows:

Multiply	By	To Obtain
cubic feet	0.02831685	cubic metres
degrees (angle)	0.01745329	radians
feet	0.3048	metres
inches	2.54	centimetres
pounds (mass)	0.4535924	kilograms
square feet	0.09290304	square metres

COUPLING HYDRODYNAMICS TO A MULTIPLE-BOX WATER QUALITY MODEL

PART I: INTRODUCTION

1. Assessment and management of water quality are aided by the use of numerical models. Water body hydrodynamics interact with biological, chemical, and other physical processes to affect water quality variables. Many simplifying assumptions are typically made in the equations governing these processes in order to develop economical numerical models. These assumptions are made in relationship to a particular situation (i.e., an assumption that might be acceptable for analyzing a problem in one water body might provide fallacious results in another).

2. One of the most routinely used assumptions suppresses variation of the variables within a cross section, and the model equations are written in a one-dimensional, longitudinal form. Typically, the cross-sectionally averaged approach is used for riverine applications. For a few well-mixed homogeneous estuaries, this approach may also be appropriate. Reservoir models sometimes assume no variation in the horizontal dimension and solve the one-dimensional, vertical form of the equation. One-dimensional models such as CE-QUAL-R1, a vertical reservoir model (Environmental Lab (EL) 1986) and CE-QUAL-RIV1, a longitudinal riverine model (EL, in preparation) solve the transport/water quality equations quickly and efficiently. The one-dimensional assumption, however, limits the problems that can be adequately addressed with these types of models. Only some reservoir problems and a very limited number of problems in estuaries and coastal embayments can be adequately addressed using this one-dimensional approach.

3. In recent years, many two-dimensional and, even more recently, three-dimensional hydrodynamic models have been developed and applied to reservoirs, estuaries, and coastal embayments. No single model can appropriately describe currents and mixing in all of these water bodies. Highly stratified estuaries require consideration of vertical variation of velocity and water quality constituents; wide estuaries require consideration of lateral variations; and large estuaries (which may be both wide and stratified) can require resolution in all three spatial dimensions. Reservoirs may be deep and stratified or broad and shallow. Because of this variety in water bodies, several different two- and three-dimensional hydrodynamic models have been developed

and used in estuarine and reservoir applications at the US Army Engineer Waterways Experiment Station (WES) by the Hydraulics Laboratory (HL) and the Coastal Engineering Research Center (CERC).

4. The necessity of evaluating environmental impacts of US Army Corps of Engineer (USACE) activities on a variety of water bodies was the impetus for the development of multidimensional water quality modeling capabilities by the EL. Three considerations guided the selection and development of a multidimensional water quality modeling approach:

- a. Long-term multidimensional water quality modeling can become cumbersome and computationally very time consuming when water quality algorithms are directly linked to hydrodynamic models.
- b. The EL should be able to perform water quality modeling studies in conjunction with hydrodynamic studies performed by both the HL and CERC.
- c. Water quality kinetics rarely require the spatial and temporal resolution required for accurate hydrodynamic calculations. To meet these requirements, a multiple-box (also known as a mixed segment, cells in series, or integrated compartment) model was chosen as the transport framework for a versatile, computationally efficient, water quality model. This type of model can be overlaid on the same grid as, or a coarser grid than, the hydrodynamic model, and it can use a larger time-step. Hydrodynamic model output can be averaged over time and space to drive the water quality model.

5. This report first describes the formulation and limitations of a multiple-box model. The Water Quality Analysis Simulation Program (WASP), developed under the auspices of the US Environmental Protection Agency (USEPA), was adapted for the purposes of this study; and the linkage of WASP to two different hydrodynamic models is described. Transport applications of the multiple-box model were made to three different water bodies with different physical characteristics: the Savannah River Estuary, DeGray Reservoir, and the Mississippi Sound. Results are analyzed and discussed.

PART II: MULTIPLE-BOX MODEL FORMULATION

General Formulation

6. WASP, the USEPA multiple-box model, was adapted for use in this study. Concentrations in this model are determined by simple mass balance around a series of completely mixed reactors, from the following equation (Ditoro, Fitzpatrick, and Thomann, 1983):

$$V_i \frac{dc_i}{dt} = \sum_j Q_{j,i} C_j + \sum_j \frac{E_{i,j} A_{i,j}}{L_{i,j}} (C_j - C_i) \pm W_i \pm K_i V_i \tag{1}$$

(1) (2) (3) (4) (5)

where

V_i = segment volume, L^3

i = segment index

j = index of adjoining segment

$Q_{j,i}$ = net advective flow from segment j to segment i, L^3/T

C_j = concentration in segment j, M/L^3

$E_{i,j}$ = dispersion coefficient for the i,j interface, L^2/T

$A_{i,j}$ = cross-sectional area of the i,j interface, L^2

$L_{i,j}$ = mixing length between segment i and j

C_i = segment concentration, M/L^3

W_i = point or distributed sources and sinks of the constituent, M/T

K_i = kinetic degradation or transformation rate, M/L^3T

This ordinary differential equation is solved in the WASP model using Euler's Method.

7. Figure 1 is a schematic illustrating the processes described by Equation 1. "A_{in}" and "A_{out}" (term 2 in Equation 1) represent the flux of material into and out of the cell by the net advection of the velocity field. "D" (term 3 in Equation 1) represents the concentration flux from some equal exchange flow between the two cells accounting for dispersive transport resulting from velocity and concentration fluctuations across the dimensions averaged. "B" (term 4 in Equation 1) is the flux of material to/from the segment boundary. "K" (term 5 in Equation 1) represents the change in

concentration arising from reactions occurring within the segment including both degradation and transformation reactions.

8. The multiple-box model is the result of a volume average for each segment of the three-dimensional advective diffusion equation; i.e., it becomes a zeroth-dimensional type equation. Individual box segments can then be arranged in any arbitrary manner forming a one-, two-, or three-dimensional network. Although Figure 1 is an example of a one-dimensional alignment of segments, the processes shown can occur between two- and three-dimensional segment arrangements as well. This geometric flexibility allows the segments to intermesh with any hydrodynamic model grid as long as box volumes and flows between the boxes can be calculated.

Dispersive Properties

9. Dispersion presents the most difficulty in the application of the multiple-box model. Two major problems arise regarding dispersion in the application of the multiple-box model. First, calculation of an appropriate dispersion coefficient for use in the multiple-box model is difficult. Second, the multiple-box model may be numerically overdiffusive. The numerical diffusion introduced by the solution technique may be greater than the physical dispersion of the system unless relatively small segments are used.

10. Calculating dispersion for any transport model is difficult. In a dimensionally averaged model, the primary contribution to dispersion arises from nonuniformity of concentration and velocity in the dimension of averaging. Although the choice of dispersion coefficients is very difficult for one- and two-dimensional estuarine transport, some systematic guidelines are available in the literature (Fischer 1976 and Fischer et al. 1979). For the multiple-box model, no systematic guidelines are available in the literature for estimating these parameters.

11. However, one potential procedure for adjustment of the dispersion coefficient is based on duplicating dye transport simulated with the hydrodynamic model. Typically, if the multiple-box model is used in conjunction with a multidimensional hydrodynamic model, the hydrodynamic model will include a transport algorithm for calculating salinity in an estuary or temperature in a reservoir. Hydrodynamic/transport models are generally calibrated against field measurements of salinity and/or temperature distribution or a dye study

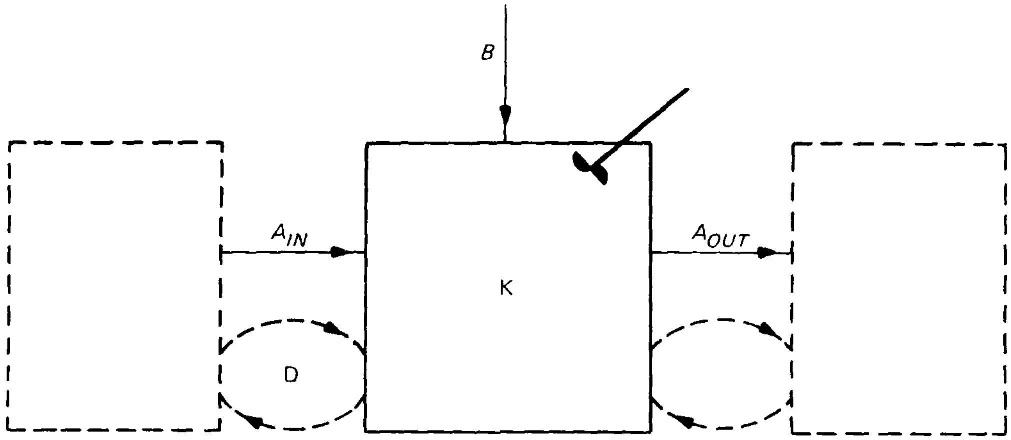

Figure 1. Schematic representation of box model processes

in the water body. Injection and transport of a conservative tracer in the hydrodynamic model, compared with the transport of an identical injection in the multiple-box model over a short period of time (i.e., a period of time typical for the hydrodynamic model runs), can be used as a guide for the adjustment of the dispersion coefficient in the multiple-box model. Additionally, this procedure would be effective in assessing the errors introduced in the use of tidally averaged values for advective transport.

12. Excessive numerical diffusion is often a critical limitation in the multiple-box concept. Shanahan and Harleman (1984) evaluated the diffusive properties of a multiple-box model using a one-dimensional arrangement of boxes, compared with a one-dimensional advective dispersion model for steady uniform flow

$$A\frac{\partial C}{\partial t} + Q\frac{\partial C}{\partial x} = A\frac{\partial}{\partial x} D\frac{\partial C}{\partial x} \qquad (2)$$

where

A = cross-sectional flow area, M^2

Q = system through flow, M^3/T

x = the coordinate in the direction of flow, L

D = one-dimensional dispersion coefficient, M^2/T

Their analysis is based on conceptual reactor models used in sewage treatment plant design. A peclet number (Pe) is defined as

$$Pe = \frac{QX}{AD} \tag{3}$$

where X is the total length of the system in the direction of flow. Their analysis indicates that, to keep the box model from being inherently over-diffusive, there must be at least n segments where n is defined as (for n being a large number)

$$n = \frac{Pe}{2} \tag{4}$$

They point out that for a given spatial step size, $\Delta x = X/n$, Equation 4 is equivalent to numerical diffusion in an upwind spatial finite difference approximation of Equation 2, i.e., $D_n = U\,x/2$, where D_n is the numerical diffusion coefficient introduced by the solution scheme and U is the cross-sectionally averaged velocity (L/T).

13. However, according to Roache (1982), numerical diffusion for upwind differencing in a one-dimensional system is of the form

$$D_n = \frac{U\Delta x}{2}(1 - \alpha) \tag{5}$$

where

$$\alpha = \frac{U\Delta t}{\Delta x}$$

Δt = time

α is referred to as the Courant number. As the Courant number approaches one, numerical diffusion approaches zero. The condition where $\alpha = 1$ is the stability limit for the upwind differencing scheme. In a one-dimensional system when $\alpha = 1$, then the value of Δt represents the time that it takes for a particle to travel the length of a cell (Δx). This stability criterion applied to the box model takes the form $Q_{ij}\Delta t/V_i = 1$ and can be interpreted

as the total flow into or out of a segment during a time-step must not exceed the volume of the segment. This interpretation lends itself to extrapolation to multidimensional problems. Restating Equation 5 in terms of multiple-box model parameters, numerical diffusion D_n at each segment interface in the multiple-box model can be described for equal length segments by

$$D_n = \frac{Q_{i,j} L_{i,j}}{2A_{i,j}} \; 1 - \frac{Q_{i,j} \Delta t}{V_i} \tag{6}$$

One-Dimensional Example

14. The transport properties of the multiple-box model are illustrated by considering steady uniform flow in a rectangular channel with the following characteristics:

H = 1.0 ft*

W = 20.0 ft

L = 2,000 ft

U = 0.2 fps

Mn = 0.017

D = 14.7 ft^2/sec

A = 20.0 ft^2

Q = 4.0 cfs

Pe = 27.2, peclet number

where H is the channel depth, W is the channel width, L is the total channel length, U is the average longitudinal velocity, and Mn is Manning's roughness coefficient. The dispersion coefficient, D , was calculated using the method of Fischer et al. (1979). For a very small time-step $\alpha \ll 1$, the channel must be divided into at least 14 segments ($n > Pe/2$) to avoid excessive numerical diffusion in the model.

---

* A table of factors for converting non-SI units of measurement to SI (metric) units is presented on page 3.

15. The effect of increasing the time-step on numerical diffusion in the box model is illustrated in Figure 2. For an initial concentration of 10 mg/ℓ in the most upstream box, concentration versus time profiles in box 13 calculated with four time-steps ranging from 0.001 to 0.0082 days are shown in this figure. No physical dispersion was input for these test cases. Numerical diffusion decreases as the time-step increases, dropping dramatically as the time-step limit ($\Delta t = 0.008275$ days) is approached. This behavior is consistent with Equation 6.

16. The box model results were compared with the analytical solution of the one-dimensional advective diffusion equation for an instantaneous point source of material injected into steady flow in a uniform channel. The solution is given by Crank (1984):

$$C(x,t) = \frac{M}{A\sqrt{4\pi Dt}} \exp \frac{-x^2}{4Dt} \tag{7}$$

where x is the downstream distance from the point of injection, t is the time since the injection, M is the mass injected, and D is the one-dimensional dispersion coefficient. Figure 3 shows the results for an injection of $M = 809$ g (the amount of mass equal to 10 mg/ℓ injected into segment 1 of the 14-segment box model discretization) injected at $x = 0$, $t = 0$, and a value of 14.7 ft^2/sec for the dispersion coefficient D compared with a 14-segment box model simulation using a 0.001-day time-step. The numerical diffusion for the box model simulation was calculated as 12.6 ft^2/sec. A value of 2.1 ft^2/sec was input for the dispersion coefficient in the model to give a total model dispersion of 14.7 ft^2/sec. Peak concentrations are slightly lower in the upstream segments of the multiple-box model since the initial mass injection must be spread over the entire box, rather than being a true point source injection. This difference is reduced at the end of the channel, and box model transport approaches the analytical solution.

Model Modifications

17. WASP was developed for lake applications using constant volume boxes and steady flows. The constant volume and steady flow assumptions are not acceptable for intratidal estuarine applications; i.e., the time-step is

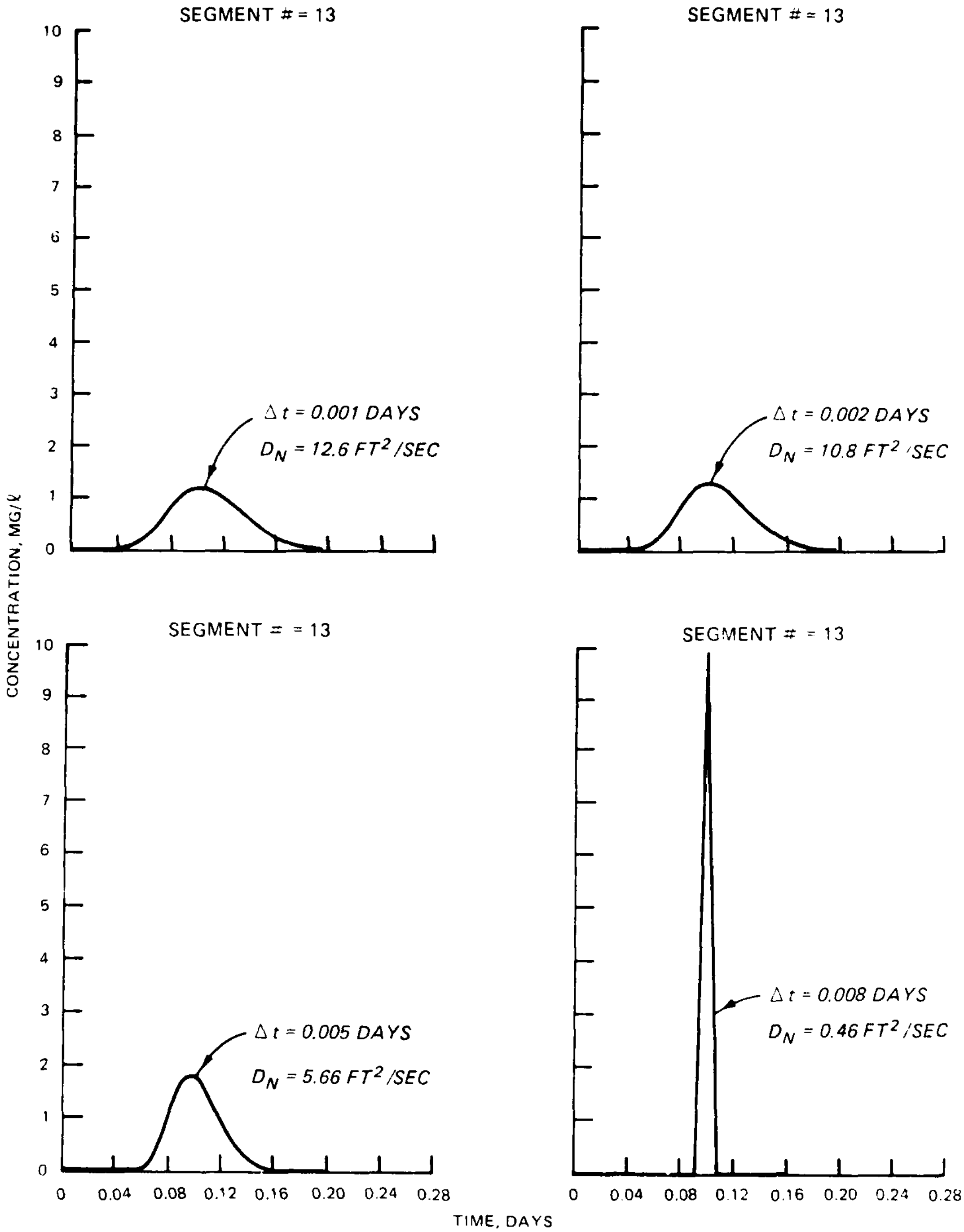

Figure 2. Effect of time-step on dispersion in the box model for a one-dimensional channel

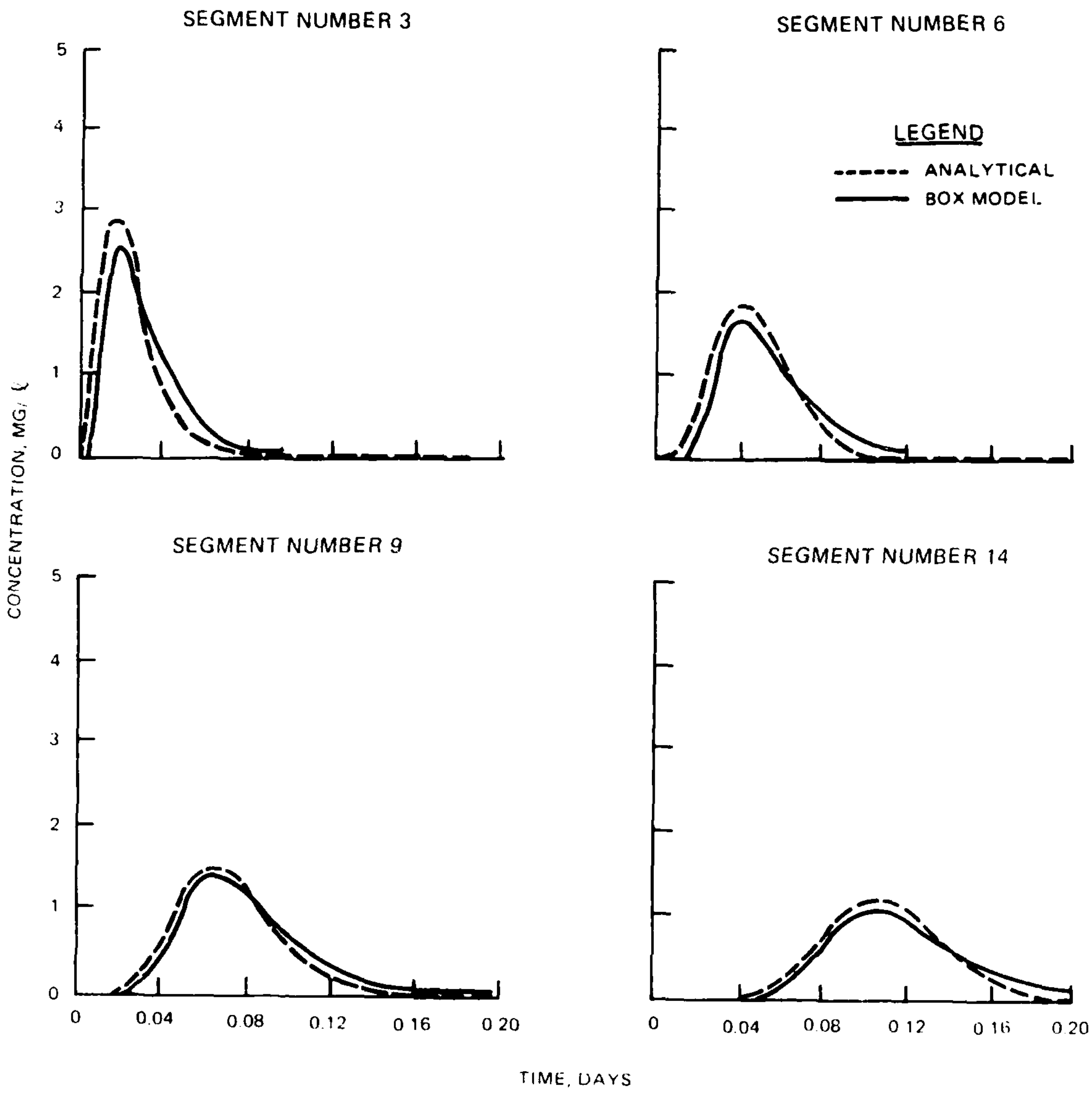

Figure 3. Comparison of box model solution to analytical solution for flow in a one-dimensional channel

less than a tidal cycle. For variable volume applications, the volume on the left hand side of Equation 1 must be written within the time differential, i.e., $D(V_iC_i)/dt$. The value for the quantity V_iC_i was found using a Euler solution scheme and solving for the concentration at the new step. The modified formulation conserves mass for both constant and variable volume applications. For variable volume/unsteady flow applications, the model must be altered to read values for volumes and flows at every computational time rather than to read them once during the initial data input.

PART III: HYDRODYNAMIC INTERFACING

General

18. In this study, the multiple-box model is interfaced with hydrodynamic output generated by two different models. The first is CE-QUAL-W2, a two-dimensional, laterally averaged hydrodynamic model developed for the USACE (EL and HL 1986). This model was originally developed for two-dimensional reservoir modeling and extended for use in deep, narrow, stratified estuaries with the addition of estuarine boundary conditions (Edinger and Buchak 1981). Applications of the Savannah River Estuary (Hall 1987) and DeGray Lake (Martin 1987) are used herein as case studies for utilization of CE-QUAL-W2 output as the hydrodynamic driver of a multiple-box model.

19. The second model used to generate hydrodynamic output for the multiple-box model in this study is WIFM-SAL (WES Implicit Flooding Model with constituent transport) (Schmalz 1985b), a vertically averaged model employing an exponentially stretched grid. WIFM-SAL was developed for the analysis of shallow estuaries and embayments that could be assumed to be vertically well mixed. An application of WIFM-SAL to the Mississippi Sound and adjacent areas (Schmalz 1985a) was used as the test case for the interface with the multiple-box model.

Interface with CE-QUAL-W2

Savannah River application

20. Figure 4 shows the computational grid for the main channel and tide gate branches for the application of CE-QUAL-W2 to the Savannah River Estuary with the multiple-box model segments overlaid on it. A relatively coarse grid overlay of 18 box model segments was made on a total of 377 active computational cells in CE-QUAL-W2. In the upper end of the estuary where the reach is predominantly riverine and unstratified, a single vertical layer of boxes was overlaid on the CE-QUAL-W2 grid and expanded to a double layer in the partially stratified downstream sections. Thus, fine-scale vertical resolution was not maintained in this box model overlay.

21. Variables in CE-QUAL-W2 are defined as shown in Figure 5. Water surface elevation (Z), cell width (B), and constituent concentrations are

GEOMETRIC SCHEMATIZATION
SAVANNAH RIVER ESTUARY APPLICATION

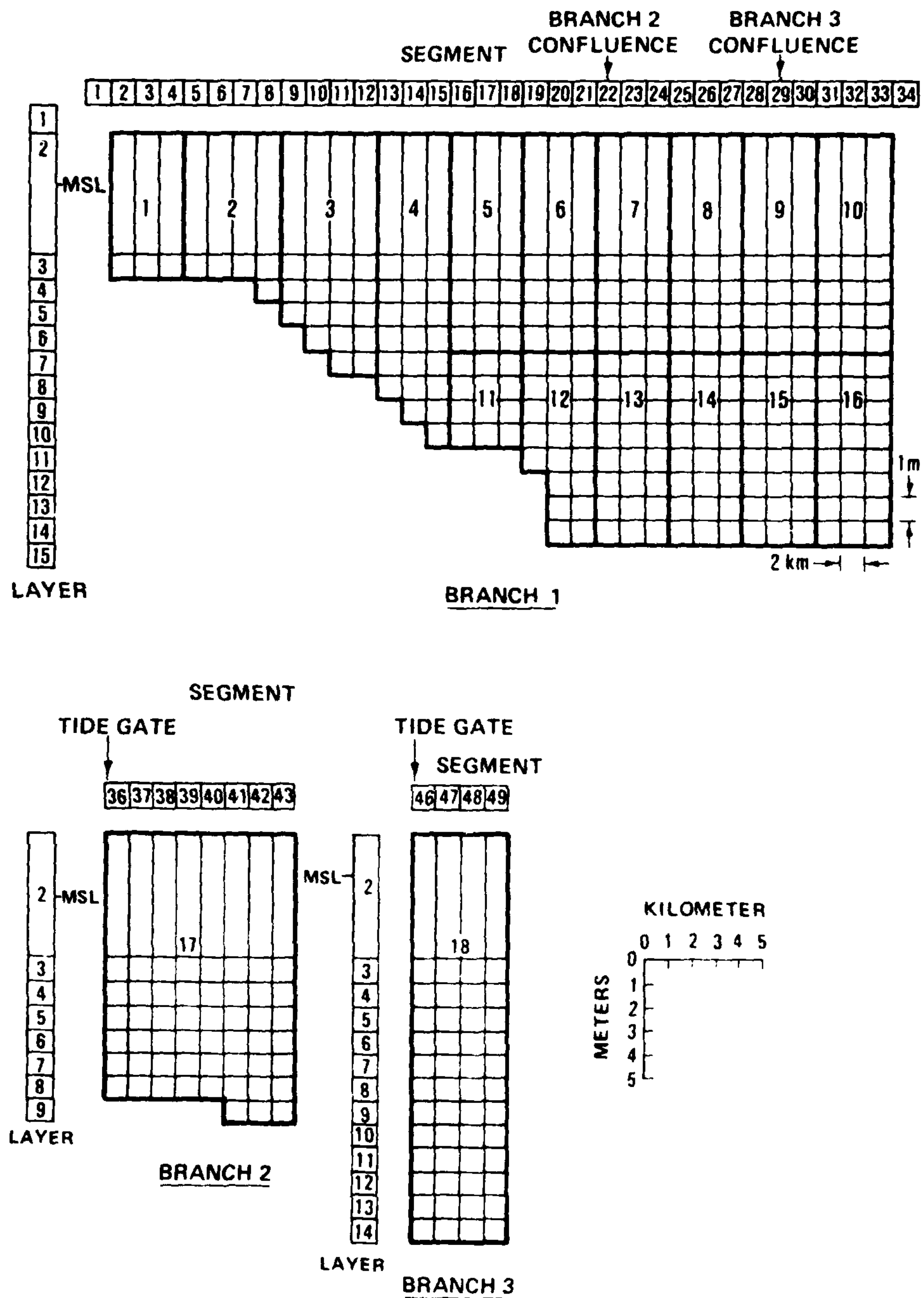

Figure 4. Savannah River Estuary grid for CE-QUAL-W2 with box model overlay shown by heavier lines

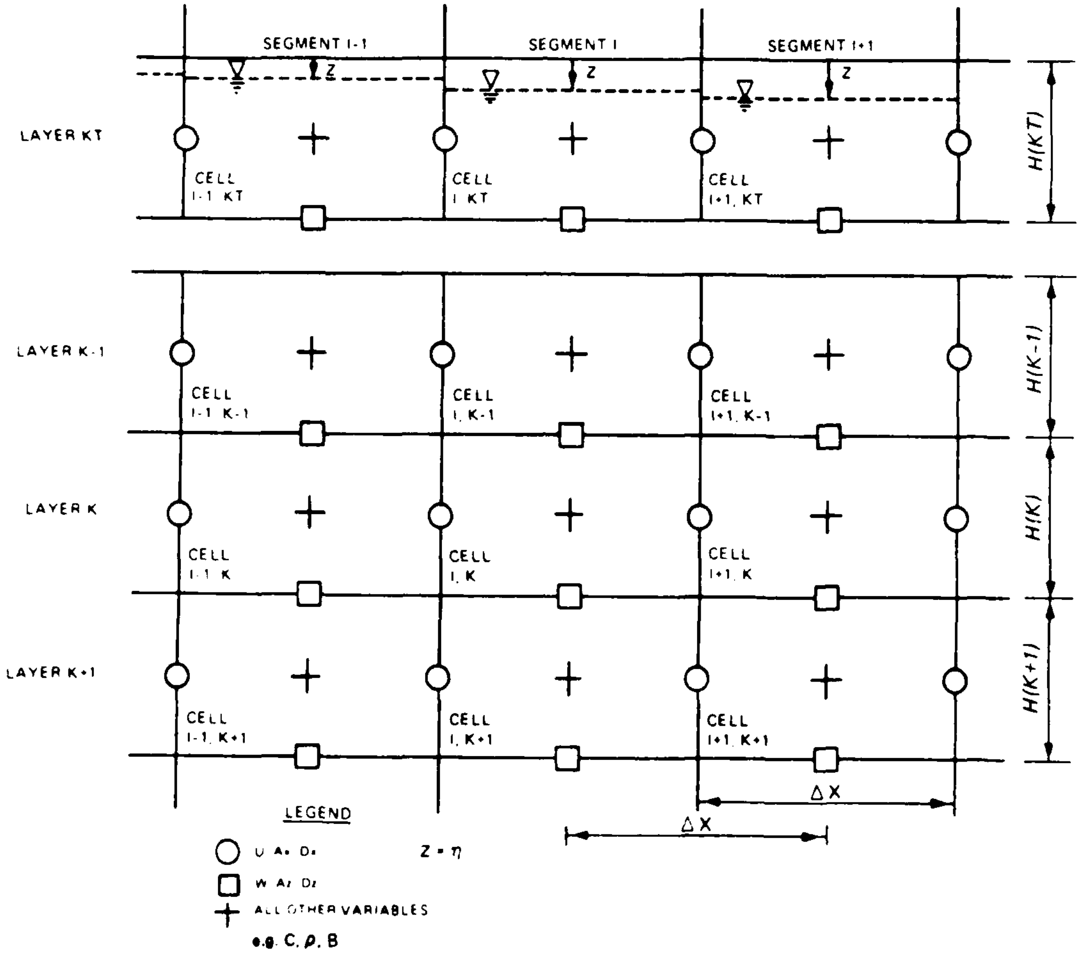

Figure 5. Variable definition sketch for CE-QUAL-W2

defined at the center of each cell. Layer thickness is a constant (H) for all except the top layer, which is variable (H-Z). Velocities (u,w) and diffusion coefficients (D_x, D_z) are defined at the cell faces.

22. Box model segment volumes were calculated at each CE-QUAL-W2 time-step by summing the CE-QUAL-W2 cell volumes within each box segment. The CE-QUAL-W2 cell volume [V(I,K)] was calculated by

$$V(I,K) = B(I,K) \times H(K) \times \Delta x \qquad K > KT$$

$$V(I,K) = B(I,K) \times [H(K) - Z(I)] \times \Delta x \qquad K = KT \qquad (8)$$

The flow across each box segment face was calculated by summing corresponding CE-QUAL-W2 cell flows at each box face. K is the layer number, and KT is the surface layer. CE-QUAL-W2 flows are given by

$$Q_h(I-1,K) = U(I-1,K) \times H(K) \times \frac{[B(I-1,K) + B(I,K)]}{2.} \qquad K \neq KT,\ I > 1$$

$$Q_h(I-2,KT) = U(I-1,KT) \times \frac{[H(KT) - Z2(I)] + [H(KT) - Z2(I-1)]}{2.}$$

$$\times \frac{[B(I-1,K) + B(I,K)]}{2} \qquad K = KT,\ I > 1$$

$$Q_v\ (I,K-1) = W(I,K-1) \times \Delta x \times \frac{[B(I,K-1) + B(I,K)]}{2} \qquad K > 1 \tag{9}$$

where Q_h and Q_v represent flows in the horizontal and vertical directions. The flow across the upstream face at $I = 1$ into the first multiple-box segment is simply the upstream boundary flow specified in CE-QUAL-W2. Box model flows are calculated by summing the flows across each of the CE-QUAL-W2 cell faces that align with the box model face.

23. The time-averaged flow ($\bar{Q}_t$) was calculated as the arithmetic average of the flows, as follows:

$$\bar{Q}_t = \sum_{n=1}^{N} \frac{Q_n}{N} \tag{10}$$

where N is the number of time-steps averaged. However, in the time-averaged data set, the volume at the beginning of each averaging interval was used since the average net flow into a segment over the averaging interval added to the volume at the beginning of the interval equalled the volume at the beginning of the next interval. In this way, continuity was assured.

DeGray Lake application

24. Whereas the Savannah River is a strongly advective system with a residence time on the order of days, DeGray Lake typically has a residence time of several months and exhibits very strong thermal stratification during the summer. Relatively fine vertical resolution is required for accurate

water quality modeling. The DeGray application of CE-QUAL-W2 used a horizontal segment length of 993.6 m and a layer thickness of 2.0 m. The first box model test used a direct grid overlay resulting in 428 segments and 828 flows. The correspondence between CE-QUAL-W2 cells and box model cells in the first box model test is shown in Table 1.

25. A second box model test consisted of a 2 by 2 overlay on the CE-QUAL-W2 grid, i.e., four CE-QUAL-W2 cells per box model segment except for some of the bottom segments. This box model application consisted of 112 segments and 210 flows. Correspondence between CE-QUAL-W2 cells and box model cells in the second box model test is shown in Table 2. Daily averaged values for flow and volume input for both of these box model overlays were calculated using the same general approach as previously described for the Savannah River application.

26. The CE-QUAL-W2 time-step for the DeGray application was 1,500 sec or 0.02+ days. The box model time-step was 0.1 day. The 1,500-sec time-step size selected for CE-QUAL-W2 reflects an internal gravity wave restriction. A subset of CE-QUAL-W2 hydrodynamic output calculated during the summer months was used for model comparisons, since interest centered primarily on erosion of the thermocline resulting from numerical diffusion in the box model. Experimentation revealed that 0.1-day time-steps were computationally stable for the box model during the time interval documented in this report; however, during autumnal overturn, the time-step size in the box model was limited to 0.02 day because of the Courant number restriction. Daily averaged values for the volumes and flows were used repeatedly for the time-steps in a particular simulation day.

Interface with WIFM-SAL

27. Figure 6 shows the transformed coordinate grid with the locations of specific variables used in WIFM-SAL calculations. The velocities (U,V) are defined at the cell faces while depth (h), water surface elevation (n), and constituent concentration are defined at the cell center. The variables α_1 and α_2 are the spatial coordinates in transformed space. Figure 7 shows the computational grid in real space coordinates for the WIFM application to the Mississippi Sound and surrounding areas. The WIFM grid is 59 by 115, i.e., nearly 7,000 cells. More boxes were needed to provide an adequate overlay on

Table 1

WASP-01 Overlay on CE-QUAL-W2 Grid*

SEGMENT NUMBER

																										28				ELEVATION, M
[illegible]	[illegible]	[illegible]	8	[illegible]	18	[illegible]	[illegible]	38	[illegible]	57	[illegible]	77	88	100	112	124	137	151	166	184	203	224	246	269	293	318	345	373	401	[illegible]
[illegible]	[illegible]	[illegible]	[illegible]	[illegible]	[illegible]	[illegible]	[illegible]	[illegible]	[illegible]	58	[illegible]	78	89	101	113	125	138	152	167	185	204	225	247	270	294	319	346	374	402	
			[illegible]	[illegible]	20	[illegible]	[illegible]	[illegible]	[illegible]	[illegible]	[illegible]	79	90	102	114	126	139	153	168	186	205	226	248	271	295	320	347	375	403	
			[illegible]	15	[illegible]	[illegible]	33	[illegible]	[illegible]	[illegible]	70	80	91	103	115	127	140	154	169	187	206	227	249	272	296	321	348	376	404	
				16	[illegible]	28	34	[illegible]	[illegible]	61	[illegible]	81	92	104	116	128	141	155	170	188	207	228	250	273	297	322	349	377	405	
				17	[illegible]	29	35	43	52	62	72	82	93	105	117	129	142	156	171	189	208	229	251	274	298	323	350	378	406	[illegible]
							36	44	53	63	73	83	94	106	118	130	143	157	172	190	209	230	252	275	299	324	351	379	407	
							37	45	54	64	74	84	95	107	119	131	144	158	173	191	210	231	253	276	300	325	352	380	408	
								46	55	65	75	85	96	108	120	132	145	159	174	192	211	232	254	277	301	326	353	381	409	
									56	66	76	86	97	109	121	133	146	160	175	193	212	233	255	278	302	327	354	382	410	
												87	98	110	122	134	147	161	176	194	213	234	256	279	303	328	355	383	411	[illegible]
													99	111	123	135	148	162	177	195	214	235	257	280	304	329	356	384	412	
																136	149	163	178	196	215	236	258	281	305	330	357	385	413	
																	150	164	179	197	216	237	259	282	306	331	358	386	414	
																		165	180	198	217	238	260	283	307	332	359	387	415	
																			181	199	218	239	261	284	308	333	360	388	416	90
																			182	200	219	240	262	285	309	334	361	389	417	
																			183	201	220	241	263	286	310	335	362	390	418	
																				202	221	242	264	287	311	336	363	391	419	
																					222	243	265	288	312	337	364	392	420	
																					223	244	266	289	313	338	365	393	421	80
																						245	267	290	314	339	366	394	422	
																							268	291	315	340	367	395	423	
																								292	316	341	368	396	424	
																									317	342	369	397	425	
																										343	370	398	426	[illegible]
																										344	371	399	427	
																											372	400	428	
																														[illegible]

* Numbers in the table indicate box model cell numbers at *CE-QUAL-W2* grid locations.

Table 2

WASP-01 Overlay on CE-QUAL-W2 Grid*

1	1	2	2	4	4	7	7	11	11	16	16	21	21	27	27	33	33	40	40	49	49	60	60	72	72	85	85	99	99
1	1	2	2	4	4	7	7	11	11	16	16	21	21	27	27	33	33	40	40	49	49	60	60	72	72	85	85	99	99
		3	3	5	5	8	8	12	12	17	17	22	22	28	28	34	34	41	41	50	50	61	61	73	73	86	86	100	100
			3	5	5	8	8	12	12	17	17	22	22	28	28	34	34	41	41	50	50	61	61	73	73	86	86	100	100
				6	6	9	9	13	13	18	18	23	23	29	29	35	35	42	42	51	51	62	62	74	74	87	87	101	101
				6	6	9	9	13	13	18	18	23	23	29	29	35	35	42	42	51	51	62	62	74	74	87	87	101	101
							10	14	14	19	19	24	24	30	30	36	36	43	43	52	52	63	63	75	75	88	88	102	102
							10	14	14	19	19	24	24	30	30	36	36	43	43	52	52	63	63	75	75	88	88	102	102
								15	15	20	20	25	25	31	31	37	37	44	44	53	53	64	64	76	76	89	89	103	103
									15	20	20	25	25	31	31	37	37	44	44	53	53	64	64	76	76	89	89	103	103
												26	26	32	32	38	38	45	45	54	54	65	65	77	77	90	90	104	104
													26	32	32	38	38	45	45	54	54	65	65	77	77	90	90	104	104
																39	39	46	46	55	55	66	66	78	78	91	91	105	105
																	39	46	46	55	55	66	66	78	78	91	91	105	105
																		47	47	56	56	67	67	79	79	92	92	106	106
																			47	56	56	67	67	79	79	92	92	106	106
																			48	57	57	68	68	80	80	93	93	107	107
																			48	57	57	68	68	80	80	93	93	107	107
																				58	58	69	69	81	81	94	94	108	108
																					58	69	69	81	81	94	94	108	108
																					59	70	70	82	82	95	95	109	109
																						70	70	82	82	95	95	109	109
																							71	83	83	96	96	110	110
																								83	83	96	96	110	110
																									84	97	97	111	111
																										97	97	111	111
																										98	98	112	112
																											98	112	112

* Numbers in the table indicate box model cell numbers at CE-QUAL-W2 grid locations.

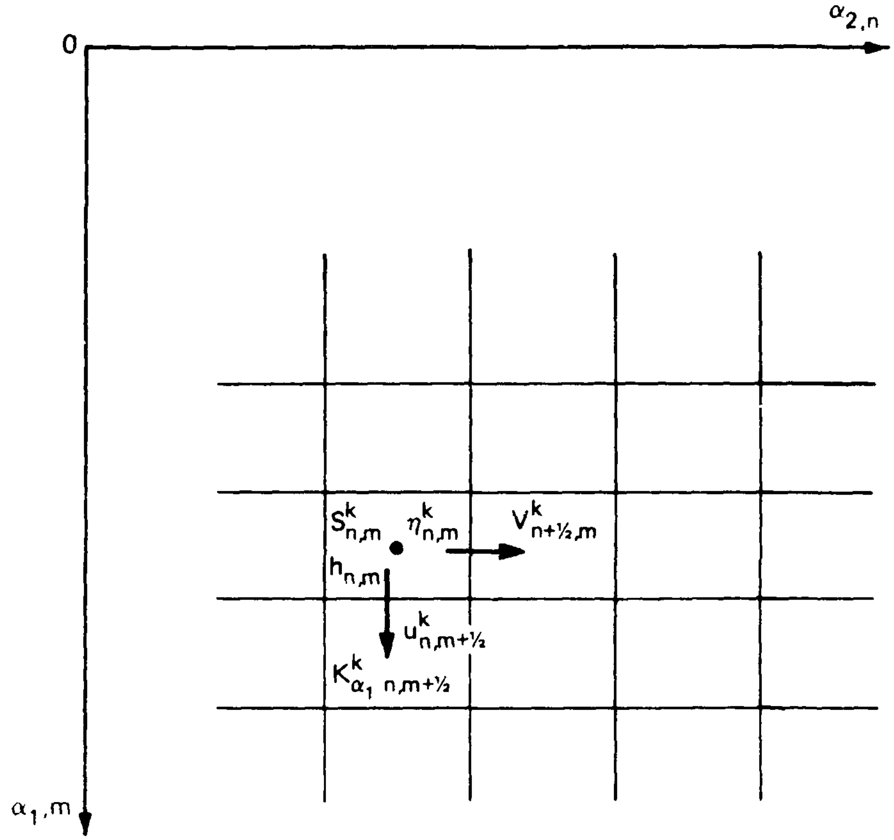

Figure 6. Variable definition sketch for WIFM

this system than were required in the Savannah River application. The overlay, selected to provide adequate resolution within the constraints of reasonable storage requirement and computation time, was a regular 2- by 3-overlay on the WIFM grid (bold outlines on Figure 7), i.e., 6:1 WIFM cells per box model segment resulting in nearly 1,000 box model segments. The use of a regular overlay made it possible to automate generation of the interface file that defined box model segments and flow faces in terms of the WIFM cells. This information is required for the generation of the box model input from hydrodynamic input. For a large number of box model cells, manual generation of this interface is tedious and time consuming.

28. An approach slightly different from that described for CE-QUAL-W2 was used in calculating volumes and flows for box model input from WIFM hydrodynamics. The solution scheme for the continuity equation employed in WIFM was used as a basis for calculation of multiple-box volumes and flows. An approach analogous to that of Schmalz (1985b) in the development of a

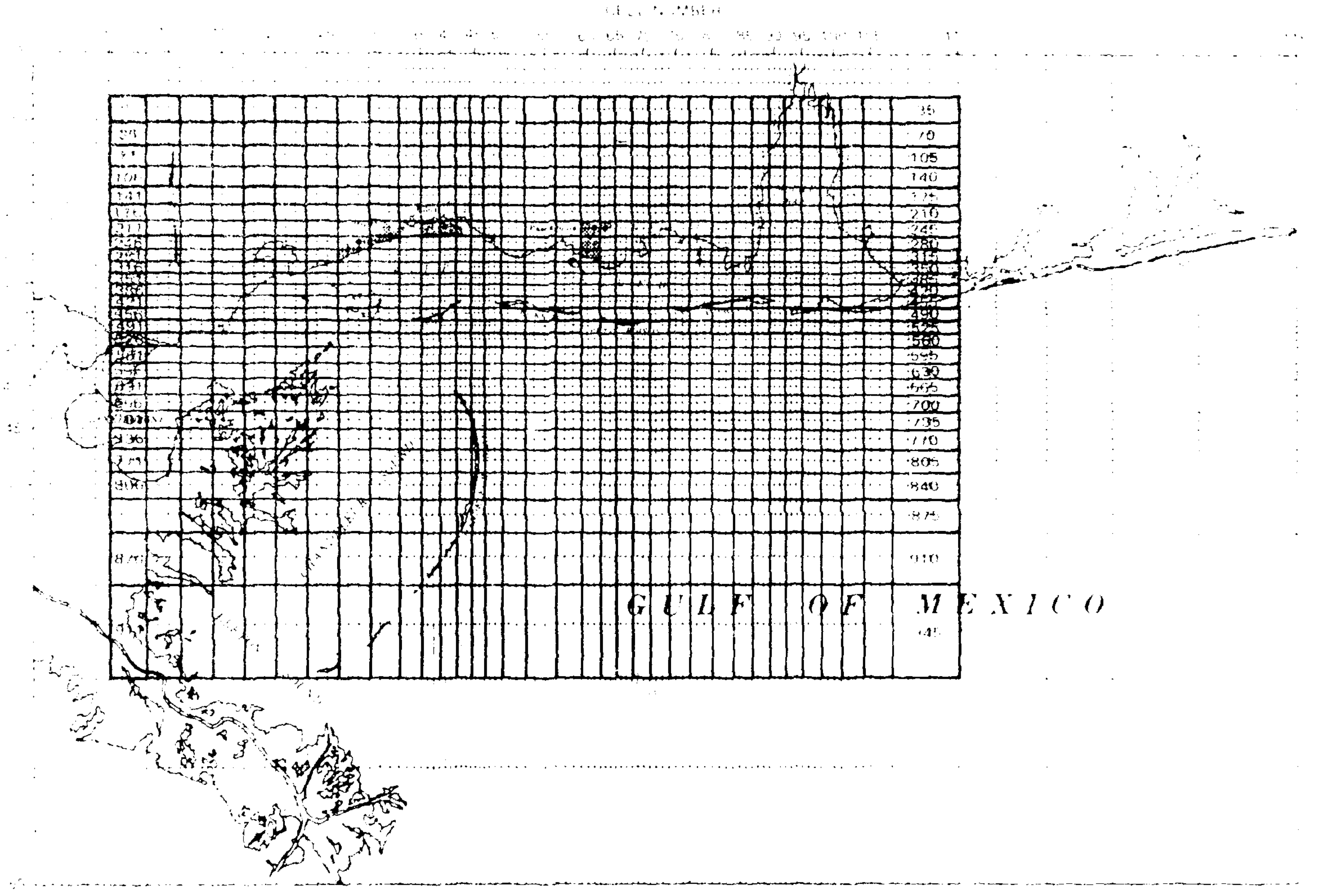

Figure 7. Mississippi Sound computational grid for WIFM-SAL with 1:6 box model overlay shown with heavy lines

three-time-level explicit transport scheme for use in WIFM-SAL was employed. The finite difference forms of the continuity equation used in the alternating difference type solution of the two-dimensional hydrodynamics were combined to yield one three-time-level finite difference expression.

$$\frac{\eta^{k+1}_{n,m} - \eta^{k-1}_{n,m}}{2\Delta t} + \frac{1}{2(\mu_1)_m \Delta\alpha_1}\left[\left(u^{k+1}_{n,m+\frac{1}{2}} + u^{k-1}_{n,m+\frac{1}{2}}\right)D^k_{n,m+\frac{1}{2}} - \left(u^{k+1}_{n,m-\frac{1}{2}} + u^{k-1}_{n,m-\frac{1}{2}}\right)D^k_{n,m-\frac{1}{2}}\right]$$

$$+ \frac{1}{2(\mu_2)_n \Delta\alpha_2}\left[\left(v^{k+1}_{n+\frac{1}{2},m} + v^{k-1}_{n+\frac{1}{2},m}\right)D^k_{n+\frac{1}{2},m} - \left(v^{k+1}_{n-\frac{1}{2},m} + v^{k-1}_{n-\frac{1}{2},m}\right)D^k_{n-\frac{1}{2},m}\right] = 0 \qquad (11)$$

with

$$D^k_{n,m\pm\frac{1}{2}} = \frac{d^k_{n,m\pm1} + d^k_{n,m}}{2}$$

$$D^k_{n\pm\frac{1}{2},m} = \frac{d^k_{n\pm1,m} + d^k_{n,m}}{2}$$

where

$\eta^{k\pm1}_{n,m}$ = water surface elevation at time level $k\pm1$ in cell (n,m)

Δt = time-step length

$(\mu_1)_m$ = stretching coefficient in α_1 direction at cell index n

$\Delta\alpha_1$ = α_1 direction space increment

$u^{k\pm1}_{n,m+\frac{1}{2}}$ = velocity component in α_1 direction for cell (n,m) at time level $k\pm1$

$(\mu_2)_n$ = stretching coefficient in α_2 direction at cell index m

$\Delta\alpha_2$ = α_2 direction space increment

$v^{k\pm1}_{n+\frac{1}{2},m}$ = velocity component in α_2 direction for cell (n,m) at time level $k\pm1$

$d^k_{n,m}$ = water depth in cell (n,m) at time level k

29. Rearranging Equation 11 and adding the time invariant depth $-h_{n,m}$ to the water surface elevation yields

$$\underbrace{\left(\eta^{k+1}_{n,m} - h_{n,m}\right)(\mu_1)_m \Delta\alpha_1 (\mu_2)_n \Delta\alpha_2}_{(1)}$$

$$= \underbrace{\left(\eta^{k-1}_{n,m} - h_{n,m}\right)(\mu_1)_m \Delta\alpha_1 (\mu_2)_n \Delta\alpha_2}_{(2)} + \underbrace{(\mu_2)_n \Delta\alpha_2 2\Delta t \left[\frac{u^{k+1}_{n,m-\frac{1}{2}} + u^{k-1}_{n,m-\frac{1}{2}}}{2}\right] D^k_{n,m-\frac{1}{2}}}_{(3)}$$

$$- \underbrace{(\mu_2)_n \Delta\alpha_2 2\Delta t \frac{\left(u^{k+1}_{n,m+\frac{1}{2}} + u^{k-1}_{n,m+\frac{1}{2}}\right)}{2.} D^k_{n,m+\frac{1}{2}}}_{(4)}$$

$$+ \underbrace{(\mu_1)_m \Delta\alpha_1 2\Delta t \frac{\left(v^{k+1}_{n-\frac{1}{2},m} + v^{k-1}_{n-\frac{1}{2},m}\right)}{2.} D^k_{n-\frac{1}{2},m}}_{(5)}$$

$$- \underbrace{(\mu_1)_m \Delta\alpha_1 2\Delta t \frac{\left(v^{k+1}_{n+\frac{1}{2},m} + v^{k-1}_{n+\frac{1}{2},m}\right)}{2.} D^k_{n+\frac{1}{2},m}}_{(6)} \qquad (12)$$

where term 1 is a finite difference expression for volume of cell (n,m) at the k+1 time level, which is set equal to the volume of the cell at the k-1 time-step (term 2), plus the net volume change resulting from the approximations for flow over two time intervals across the four faces of the cell (terms 3, 4, 5, and 6). Continuity can be guaranteed in the generation of box model parameters if calculation of volume and flow are based on Equation 12.

30. Box segment volume is calculated as the sum of the volume of the cells overlaid where individual WIFM cell volume, $Vol^{k-1}_{n,m}$, is calculated (as suggested by Equation 12) by

$$Vol^{k-1}_{n,m} = \left(\eta^{k-1}_{n,m} - h_{n,m}\right)(\mu_1)_m \Delta\alpha_1 (\mu_2)_n \Delta\alpha_2 \qquad (13)$$

Likewise, box model flows are calculated by summing the flows across each of the WIFM cell faces aligned with the box model face. The flow into each WIFM cell is found for α_1 and α_2 directions by dividing terms 3 and 5 respectively by $2\Delta t$ (terms 4 and 6 represent flow out of the WIFM cell). Since Equation 12 is a three-time-level finite difference expression, flows and volumes are calculated at alternate WIFM time-steps since terms 3 and 5 give

the flow from the $k-1$ to $k+1$ time levels and the time interval used for multiple-box input is $2\Delta t$ where Δt is the WIFM-SAL time-step. Additional time-averaging can then be performed as described for the interface with CE-QUAL-W2.

PART IV: TRANSPORT APPLICATIONS

General

31. To identify the potential and limitations for simulating multidimensional transport using the relatively coarse grid, long time-step, multiple-box model, movement of a conservative constituent in the box model was compared with movement of the same constituent in the finer scale, directly linked, transport models. Results for the box model and CE-QUAL-W2 simulations were compared using both Savannah River Estuary and DeGray Lake applications; comparison with WIFM-SAL used the Mississippi Sound application.

Comparison with CE-QUAL-W2

Savannah River application

32. A 25-mg/ℓ instantaneous dye injection was made in segment 3 of the box model and in the equivalent area of the CE-QUAL-W2 grid for the Savannah River Estuary, as shown in Figure 4. CE-QUAL-W2 hydrodynamics were averaged as described in Part III and used to drive the box model. Simulations were performed for 3.5 days. CE-QUAL-W2 simulations required a 2-min time-step, whereas the box model was run at a series of time-steps up to 3.5 hr. In order to evaluate the ability of the box model overlay to replicate CE-QUAL-W2 transport, a set of three graphical displays was made for several of the box model segments. The first graph was a time-history of the volume weighted average of the concentrations in the CE-QUAL-W2 cells contained within a given box model segment (represented in the graph by a solid line) and the range of the concentrations (shown with the vertical bar (|)) found in these cells (Figures 8a-14a). The second graph in the set was a time-history of concentrations for the 3.5-hr box model simulations (o____o) compared with the volume weighted CE-QUAL-W2 results (Δ____Δ) (Figures 8b-14b). The third graph in the set was concentration time-histories in the segment for the box model simulation using different time-step sizes (Figures 8c-14c), representing 0.5-hr (Δ____Δ), 2-hr (+____+), and 3.5-hr (o____o) time-step results, respectively.

33. The CE-QUAL-W2 cells that overlay segment 4 immediately downstream of the injection location show the greatest variation in concentration for any

of the segments (Figure 8a). The coarse box model overlay did not provide the resolution of the finer CE-QUAL-W2 grid. Excessive information was lost where the variation of concentration within the segment was large compared with the average concentration in the segment. However, the average concentration in the CE-QUAL-W2 cells and the box model simulation agree (Figure 8b) except for the concentration peak value in this segment. The peak concentration in the box model simulation was sensitive to the time-step choice (Figure 8c). For example, the 0.5-hr time-step for the box model simulation substantially decreased the peak concentration compared with the 2.0- and 3.5-hr time-steps. At segment 5, a large variation in the concentrations in the overlaid CE-QUAL-W2 cells diminished substantially downstream (Figures 9a-12a) at segments 6, 7, and 9. The box model replicated the oscillation in concentrations caused by the flow reversals. The phase as well as the magnitude of the oscillations was generally matched.

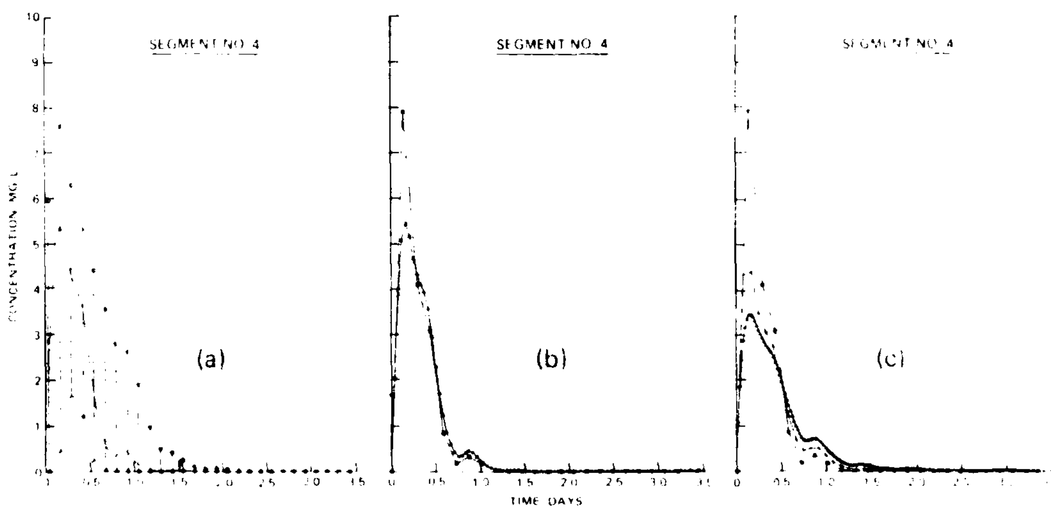

Figure 8. Savannah River application: concentration time-history for box model segment 4 and overlaid CE-QUAL-W2 cells. (a) Volume weighted average of CE-QUAL-W2 cells overlaid by the box model segment (______) and the range of concentration in these cells (|), (b) comparison of box model (o______o) and CE-QUAL-W2 (Δ______Δ) results, (c) comparison of box model results using a 0.5-hr (Δ______Δ), 2-hr (+_____+), and 3.5-hr (o______o) time-step

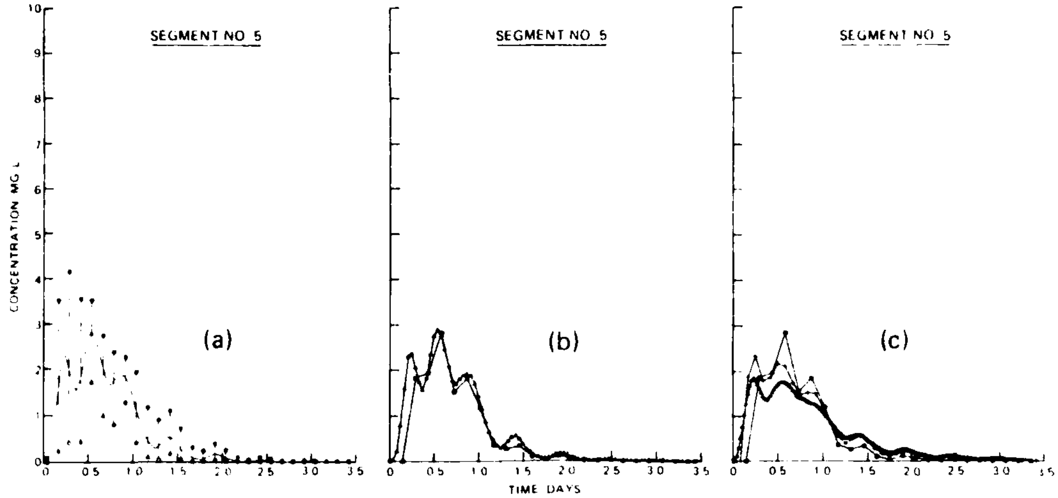

Figure 9. Savannah River application: concentration time-history for box model segment 5 and overlaid CE-QUAL-W2 cells. (a) Volume weighted average of CE-QUAL-W2 cells overlaid by the box model segment (_______) and the range of concentration in these cells (|), (b) comparison of box model (o______o) and CE-QUAL-W2 (Δ______Δ) results, (c) comparison of box model results using a 0.5-hr (Δ______Δ), 2-hr (+_____+), and 3.5-hr (o______o) time-step

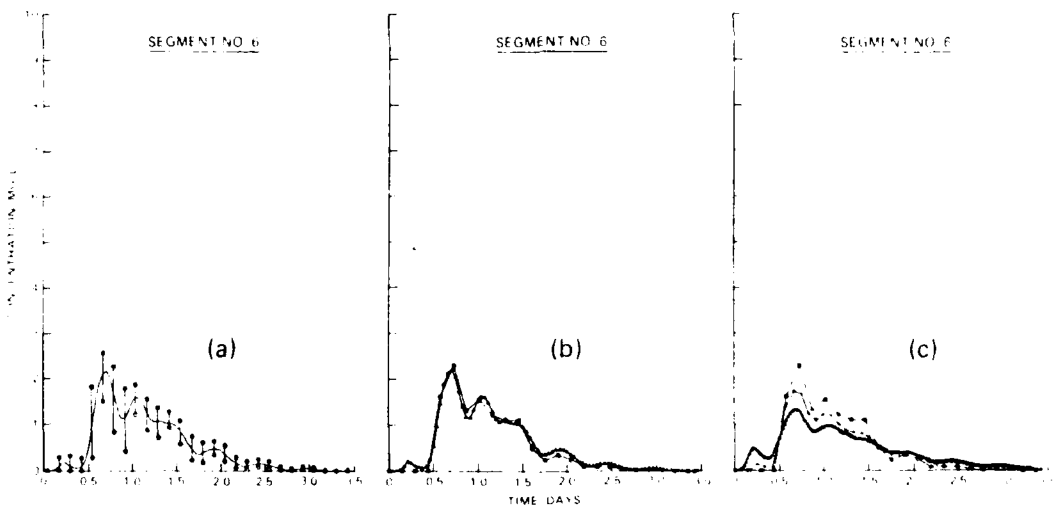

Figure 10. Savannah River application: concentration time-history for box model segment 6 and overlaid CE-QUAL-W2 cells. (a) Volume weighted average of CE-QUAL-W2 cells overlaid by the box model segment (_______) and the range of concentration in these cells (|), (b) comparison of box model (o______o) and CE-QUAL-W2 (Δ______Δ) results, (c) comparison of box model results using a 0.5-hr (Δ______Δ), 2-hr (+_____+), and 3.5-hr (o______o) time-step

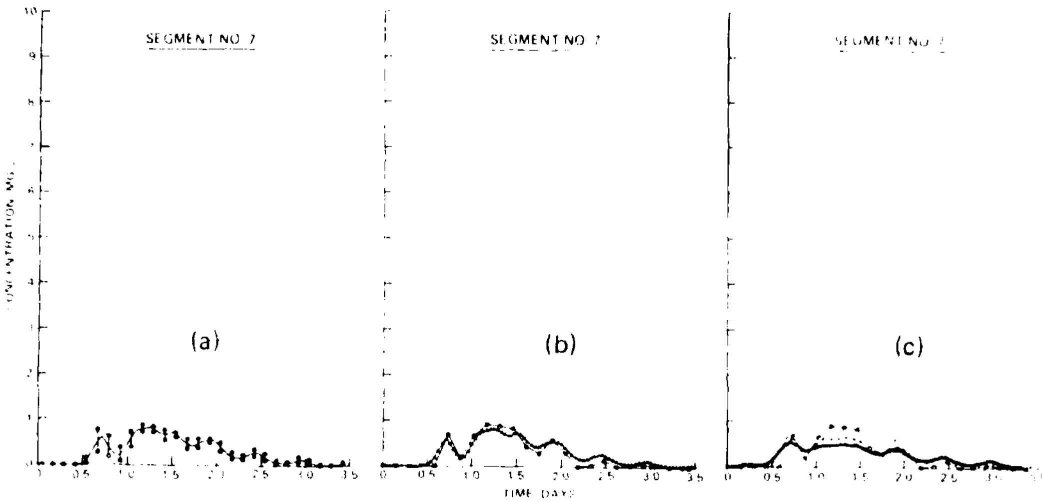

Figure 11. Savannah River application: concentration time-history for box model segment 7 and overlaid CE-QUAL-W2 cells. (a) Volume weighted average of CE-QUAL-W2 cells overlaid by the box model segment (_______) and the range of concentration in these cells (|), (b) comparison of box model (o______o) and CE-QUAL-W2 (Δ______Δ) results, (c) comparison of box model results using a 0.5-hr (Δ______Δ), 2-hr (+_____+), and 3.5-hr (o______o) time-step

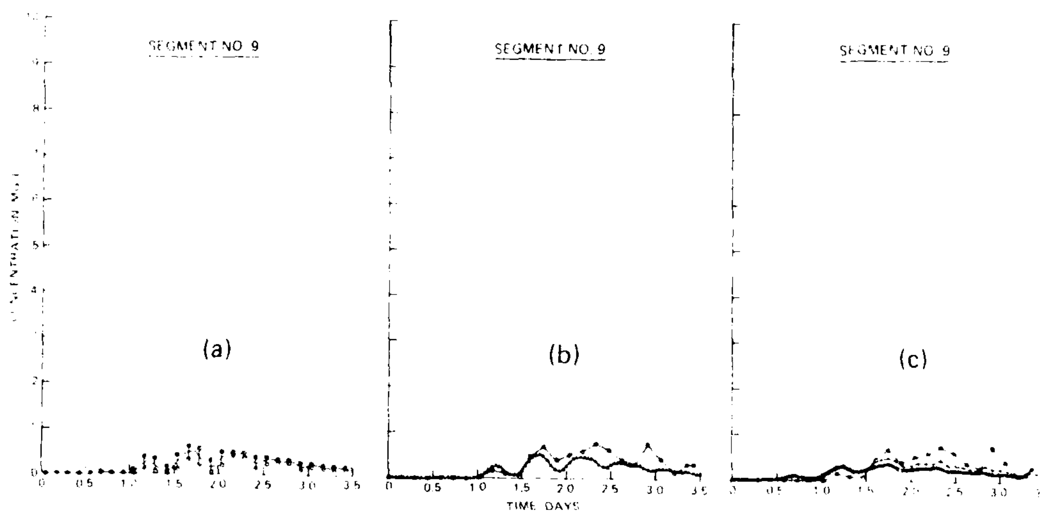

Figure 12. Savannah River application: concentration time-history for box model segment 9 and overlaid CE-QUAL-W2 cells. (a) Volume weighted average of CE-QUAL-W2 cells overlaid by the box model segment (_______) and the range of concentration in these cells (|), (b) comparison of box model (o______o) and CE-QUAL-W2 (Δ______Δ) results, (c) comparison of box model results using a 0.5-hr (Δ______Δ), 2-hr (+_____+), and 3.5-hr (o______o) time-step

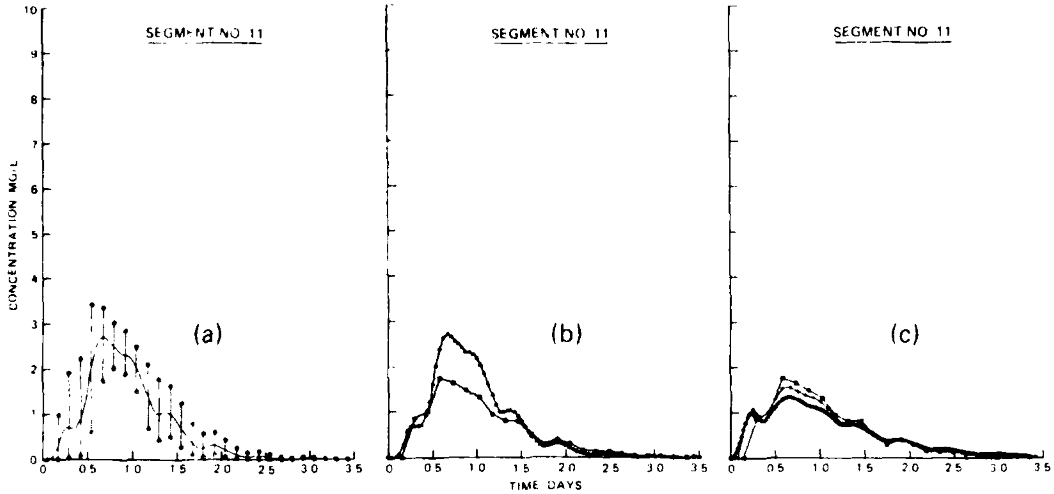

Figure 13. Savannah River application: concentration time-history for box model segment 11 and overlaid CE-QUAL-W2 cells.
(a) Volume weighted average of CE-QUAL-W2 cells overlaid by the box model segment (______) and the range of concentration in these cells (|), (b) comparison of box model (o_____o) and CE-QUAL-W2 (Δ_____Δ) results, (c) comparison of box model results using a 0.5-hr (Δ_____Δ), 2-hr (+____+), and 3.5-hr (o_____o) time-step

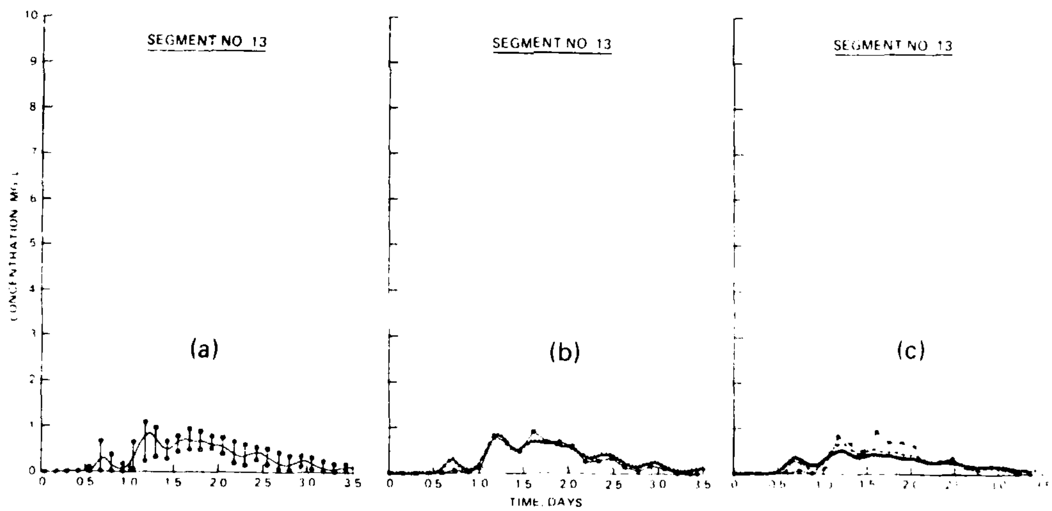

Figure 14. Savannah River application: concentration time-history for box model segment 13 and overlaid CE-QUAL-W2 cells. (a) Volume weighted average of CE-QUAL-W2 cells overlaid by the box model segment (______) and the range of concentration in these cells (|), (b) comparison of box model (o_____o) and CE-QUAL-W2 (Δ_____Δ) results, (c) comparison of box model results using a 0.5-hr (Δ_____Δ), 2-hr (+____+), and 3.5-hr (o_____o) time-step

34. However, in segment 11 (Figure 13b) the box model does not adequately simulate the average concentration in the CE-QUAL-W2 cells that it overlays. The box model underestimates the peak concentration in this segment even using the 3.5-hr time-step. The source of this error becomes clear when the large range of concentrations in the CE-QUAL-W2 cells overlaid by segment 4 (Figure 8a), the segment upstream from segment 11, is considered. Circulation in the estuary moved the highest concentration material into the bottom cells of this segment, but the box model transported the average value from segment 4 into segment 11. Given the particular box model overlay and injection condition, this anomaly was the result of lowered spatial resolution of the box model overlay. At segment 13 (Figure 14) farther downstream in the bottom layer of boxes, the box model simulation mimicked the average CE-QUAL-W2 results. The box overlay can impact accuracy of results and should be carefully considered in terms of the problems addressed. If a sharp front is not simulated, results will not be so severe.

<u>DeGray Lake application</u>

35. The primary objective of the DeGray Lake application was to compare the vertical spreading of material in the WASP grids with the CE-QUAL-W2 simulation. A uniform injection of dye was made in the top layers of both the box model and CE-QUAL-W2 grid. For the 1:1 WASP (referred to as WASP01) overlay, a 100-mg/ℓ injection was made into the surface layer of cells in both models. For the 2:1 WASP overlay (referred to as WASP02), the mass injected into the surface layer of the CE-QUAL-W2 cells was distributed through the respective WASP surface layer segments. The initial WASP02 segment tracer concentrations are listed in Table 3.

36. Daily averaged values of flows were calculated from the CE-QUAL-W2 output for WASP input; a time-step of 0.1 day was used in the WASP simulation (i.e., each set of averaged hydrodynamics was used for 10 time-steps). For the WASP01 simulation, 0.1 day approached the time-step limit; for the WASP02 simulation, a 0.5-day time-step could be used without instabilities. However, all results presented here used a 0.1-day time-step in the simulation. If simulations were carried through fall overturn, shorter time-steps had to be used, as mentioned in Part III.

37. Concentration versus elevation plots at six longitudinal segments after 30, 60, and 90 days of simulation are shown respectively in Figures 15-17. In these figures, TEST01 refers to the concentration in the

Table 3

Initial WASP02 Segment Tracer Concentrations (mg/ℓ)

Layer No.	WASP02 Segments														
	1	2	3	4	5	6	7	8	9	10	11	12	13	14	15
1	78.91	78.70	68.94	67.01	67.55	66.65	67.90	69.98	67.59	67.49	65.60	66.97	68.47	65.55	64.43
2		0.00	0.00	0.00	0.00	0.00	0.00	0.00	0.00	0.00	0.00	0.00	0.00	0.00	0.00
3			0.00	0.00	0.00	0.00	0.00	0.00	0.00	0.00	0.00	0.00	0.00	0.00	0.00
4				0.00	0.00	0.00	0.00	0.00	0.00	0.00	0.00	0.00	0.00	0.00	0.00
5					0.00	0.00	0.00	0.00	0.00	0.00	0.00	0.00	0.00	0.00	0.00
6							0.00	0.00	0.00	0.00	0.00	0.00	0.00	0.00	0.00
7									0.00	0.00	0.00	0.00	0.00	0.00	0.00
8										0.00	0.00	0.00	0.00	0.00	0.00
9										0.00	0.00	0.00	0.00	0.00	0.00
10											0.00	0.00	0.00	0.00	0.00
11											0.00	0.00	0.00	0.00	0.00
12												0.00	0.00	0.00	0.00
13													0.00	0.00	0.00
14														0.00	0.00

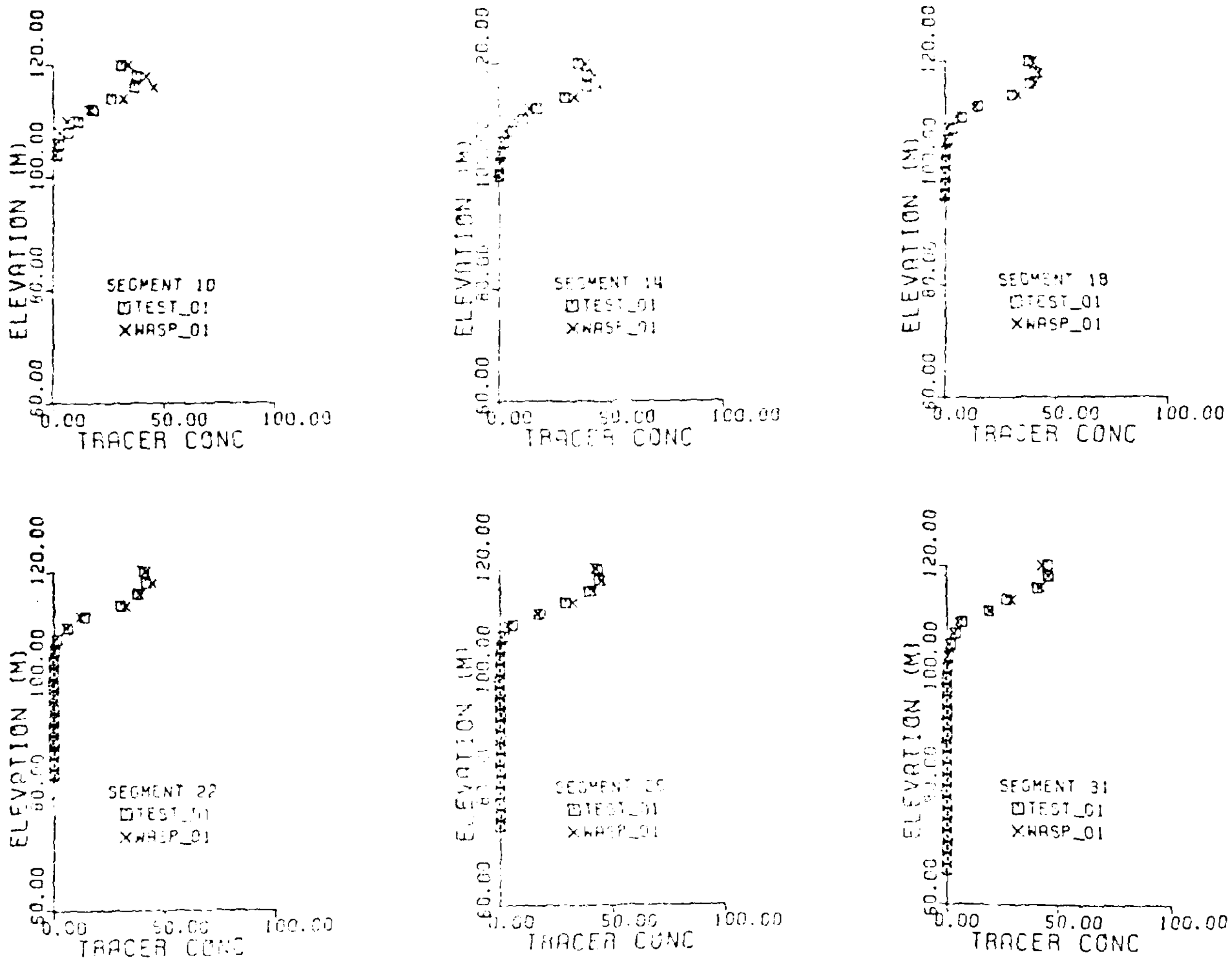

Figure 15. DeGray Lake WASP01 test results compared with CE-QUAL-W2 results after 30-day simulation

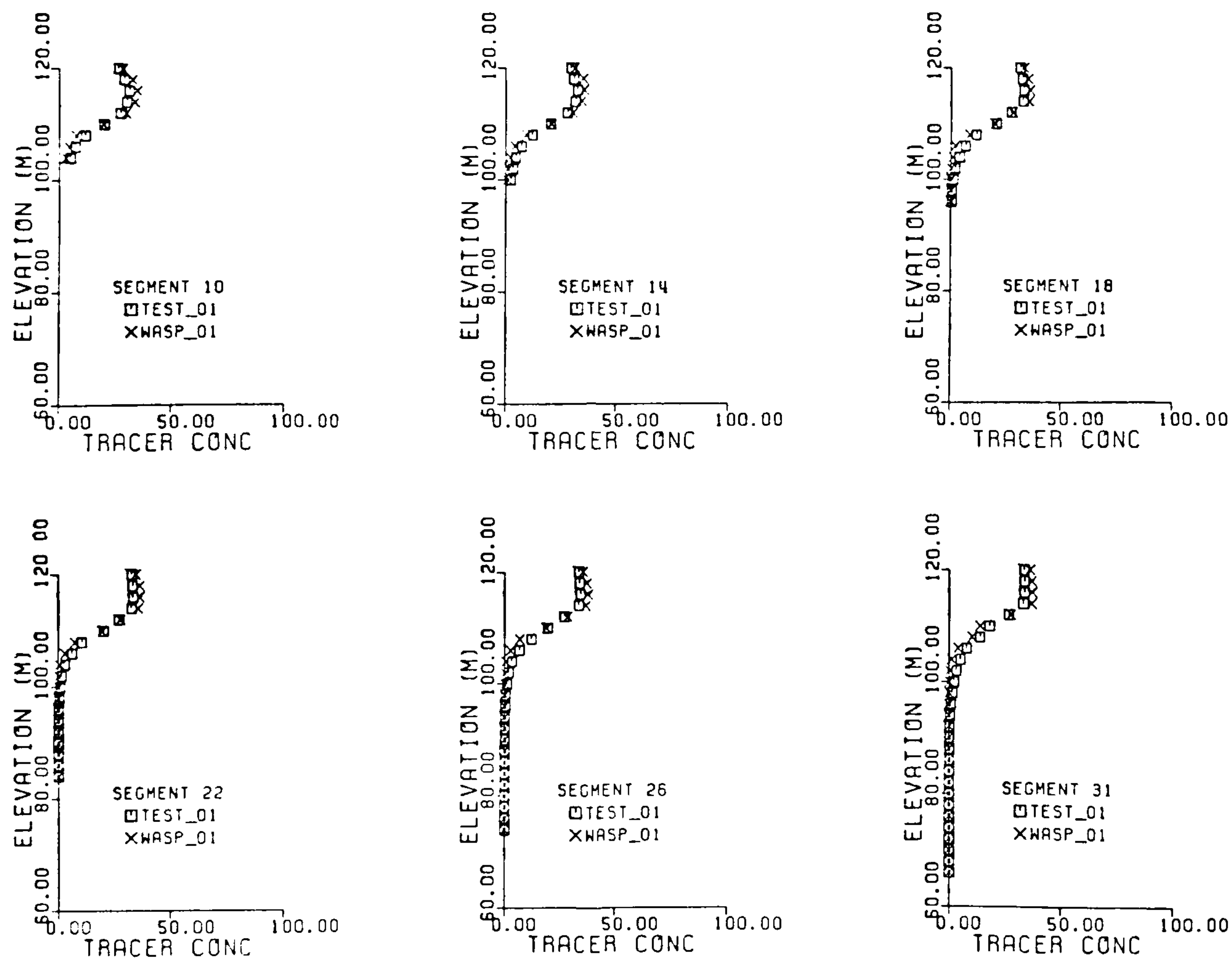

Figure 16. DeGray Lake WASP01 test results compared with CE-QUAL-W2 results after 60-day simulation

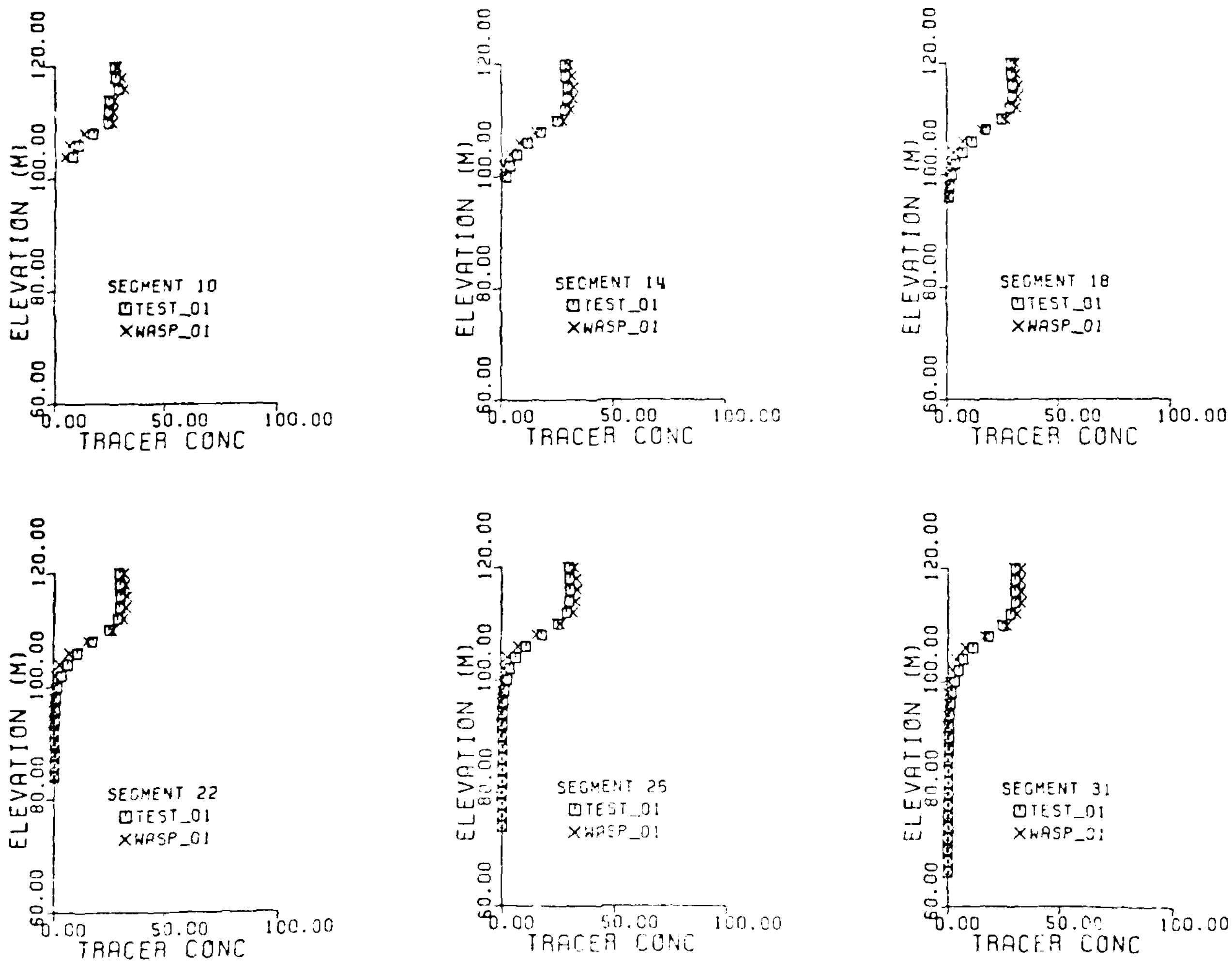

Figure 17. DeGray Lake WASP01 test results compared with CE-QUAL-W2 results after 90-day simulation

overlaid CE-QUAL-W2 cells. Results were very similar for the WASP01 and TEST01 simulations. WASP01 was slightly less vertically diffusive than TEST01. Numerical diffusion may be slightly lower for WASP01 because of the larger time-step. While the CE-QUAL-W2 simulation required over 2 hr of simulation time, the WASP01 required less than 4 min.

38. Similar plots were prepared for the WASP02 simulation (Figures 18-20). In these plots, the TEST02 values refer to the volume weighted average of the concentrations in the CE-QUAL-W2 cells overlaid by the WASP segments. After 30 days of simulation (Figure 18), concentration differences in the upper layers were significant. The greatest deviation between the two simulations occurred in the upper layers. A large portion of this deviation was probably due to the fact that the initial box concentrations represented a distribution of surface CE-QUAL-W2 cell tracer mass over two layers. By 60 days (Figure 19), the tracer was generally mixed through the epilimnion in both cases, and the only remaining significant deviation was in the metalimnion at the segment near the dam. This trend continued, and at 90 days, the deviation, even in the downstream segment, was further reduced. The increased concentration observed for WASP02 in segment 5 between 30 and 60 days was due to reversed surface currents. The VAX 11/750 CPU time requirement for the WASP02 simulation was approximately 1 min.

Comparison with WIFM-SAL

39. Two different injections were made into the 6:1 box model grid overlay and in the analogous areas of the WIFM-SAL grid. First, a 25-mg/ℓ spike was made in segment 683 of the WASP model (see Figure 7) and the six corresponding cells for the WIFM-SAL simulation. Second, a gradient-type initial condition was input in both WASP and WIFM-SAL. Initial concentrations for this injection are tabulated by box number in Table 4 and shown as a contour plot in Figure 21. For a direct (1:1) box model grid overlay of the Mobile Bay area, a 25-mg/ℓ dye injection was made at WIFM-SAL grid location N = 95, M = 8 (see Figure 7).

40. Results for these test cases are presented as contour plots after 4.5 days of simulation. The large number of grid points and box segments made plotting individual segment concentration histories unwieldy. Concentration contours of WIFM-SAL results after 4.5 days of simulation for the 25-mg/ℓ

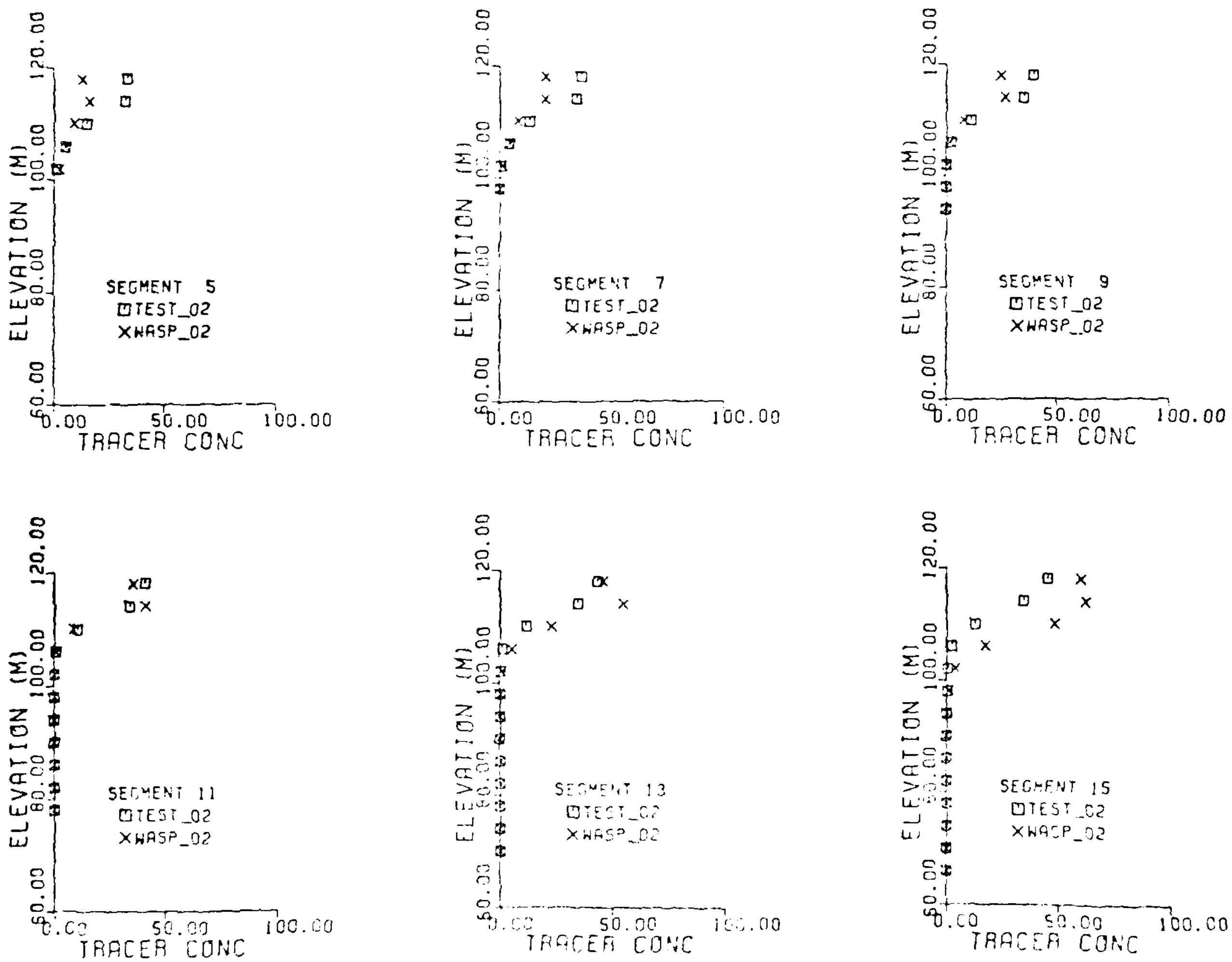

Figure 18. DeGray Lake WASP02 test results compared with CE-QUAL-W2 results after 30-day simulation

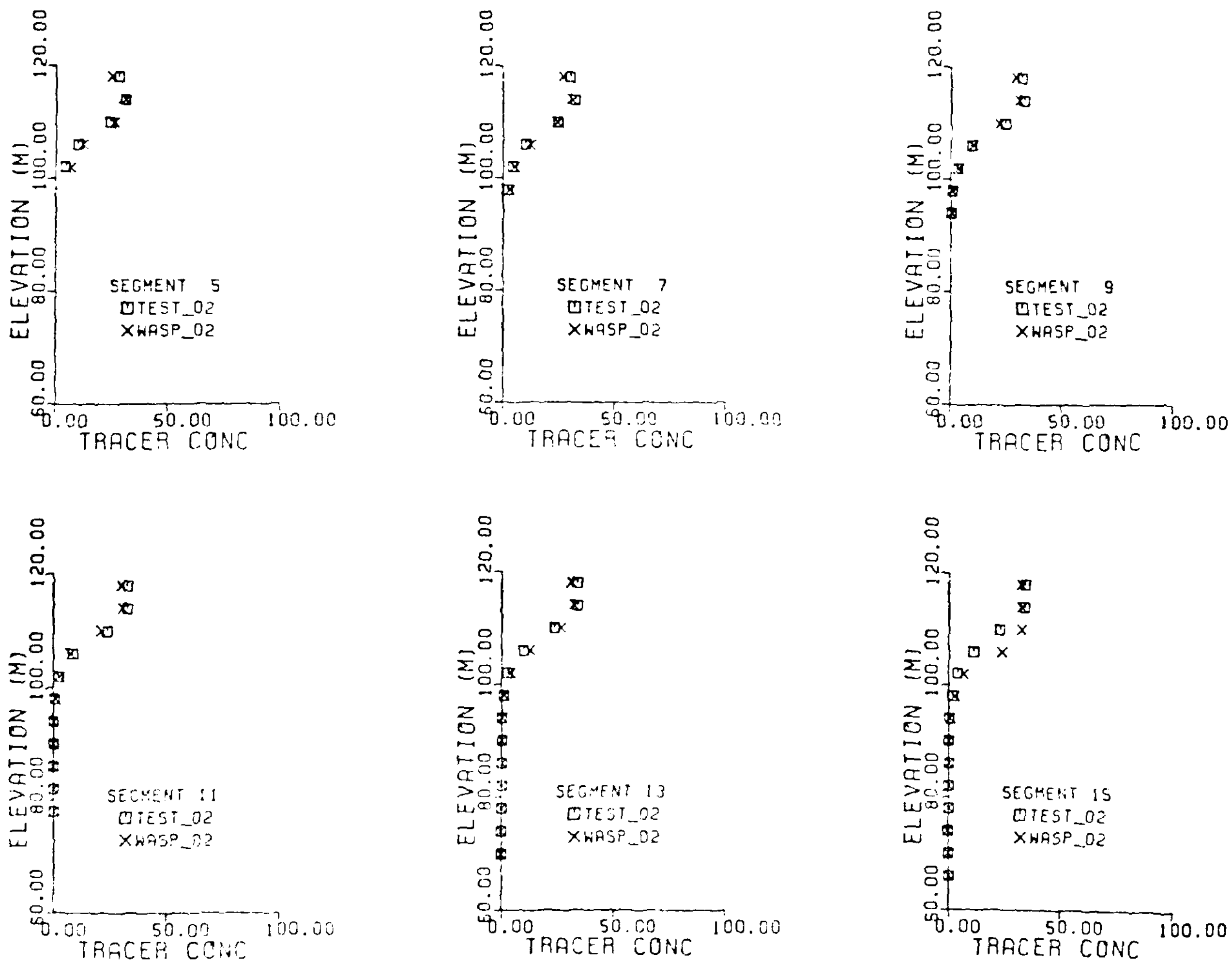

Figure 19. DeGray Lake WASP02 test results compared with *CE-QUAL-W2* results after 60-day simulation

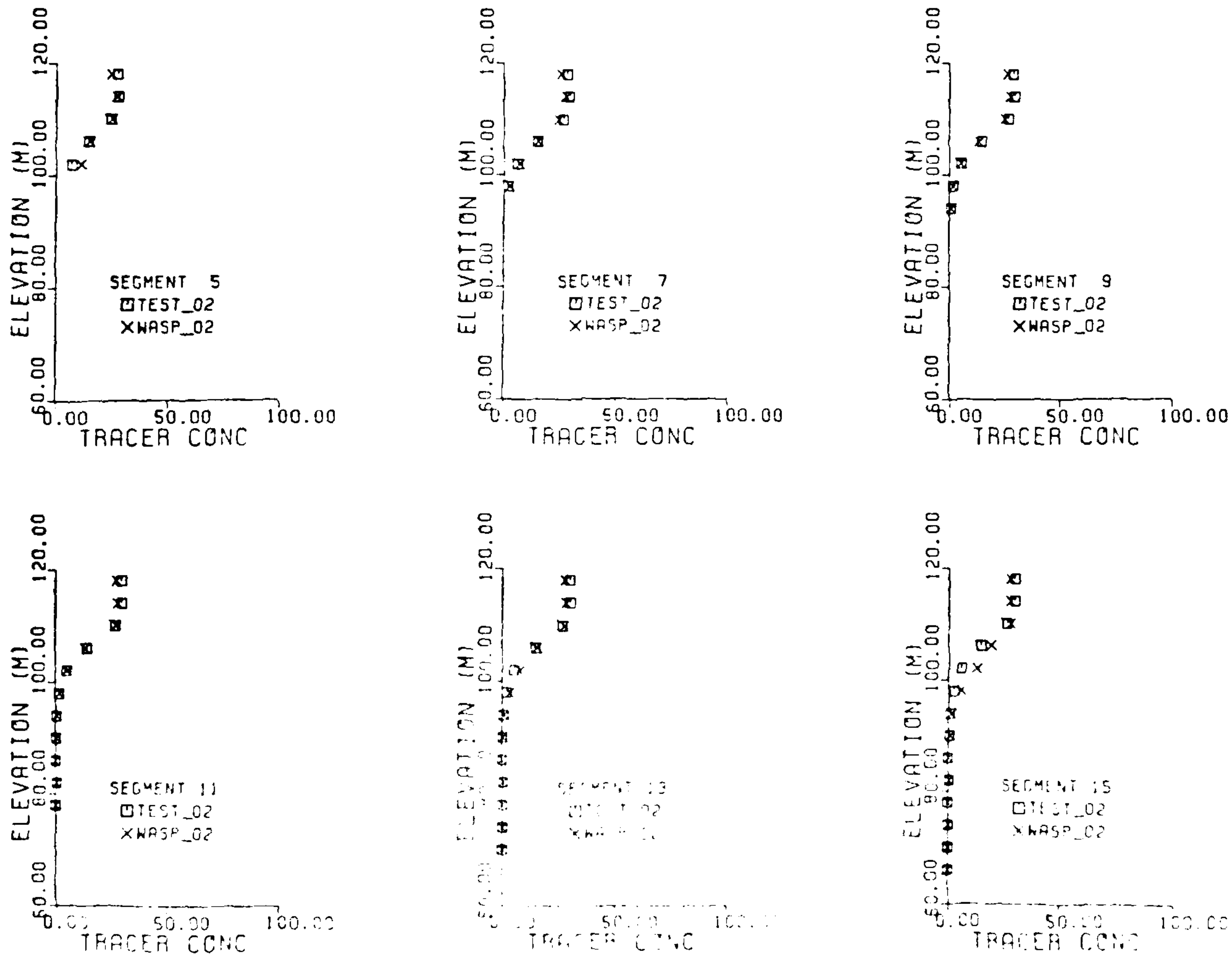

Figure 20. DeGray Lake WASP02 test results compared with CE-QUAL-W2 results after 90-day simulation

Table 4

WASP Gradient Injection, Initial Concentrations, Mississippi Sound

Box No.	Conc mg/ℓ	Box No.	Conc mg/ℓ	Box No.	Conc mg/ℓ
432	0.1	557	5.0	721	5.0
433	0.1	558	5.0	722	1.0
434	0.1	559	5.0	723	0.5
435	0.1	580	5,0	724	0.1
436	0.1	581	3.0	747	0.1
437	0.1	582	1.0	748	0.5
438	0.1	583	0.5	749	1.0
439	0.1	584	0.1	750	3.0
440	0.1	607	0.1	751	3.0
441	0.1	608	0.5	752	3.0
442	0.1	609	1.0	753	3.0
443	0.1	610	3.0	754	3.0
444	0.1	611	5.0	755	3.0
467	0.1	612	7.0	756	3.0
468	0.5	613	7.0	757	1.0
469	0.5	614	7.0	758	0.5
470	0.5	615	5.0	759	0.1
471	0.5	616	3.0	782	0.1
472	0.5	617	1.0	783	0.5
473	0.5	618	0.5	784	1.0
474	0.5	619	0.1	785	1.0
475	0.5	642	0.1	786	1.0
476	0.5	643	0.5	787	1.0
477	0.5	644	1.0	788	1.0
478	0.5	645	3.0	789	1.0
479	0.1	646	5.0	790	1.0
502	0.1	647	7.0	791	1.0
503	0.5	648	9.0	792	1.0
504	1.0	649	7.0	793	0.5
505	1.0	650	5.0	794	1.0
506	1.0	651	5.0	817	0.1
507	1.0	652	1.0	818	0.5
508	1.0	653	0.5	819	0.5
509	1.0	654	0.1	820	0.5
510	1.0	677	0.1	821	0.5
511	1.0	678	0.5	822	0.5
512	1.0	679	1.0	823	0.5
513	0.5	680	3.0	824	0.5
514	0.1	681	5.0	825	0.5
537	0.1	682	7.0	826	0.5
538	0.5	683	7.0	827	0.5
539	1.0	684	7.0	828	0.5
540	3.0	685	5.0	829	0.1
541	3.0	686	3.0	852	0.1
542	3.0	687	1.0	853	0.1
543	3.0	688	0.5	854	0.1
544	3.0	689	0.1	855	0.1
545	3.0	712	0.1	856	0.1

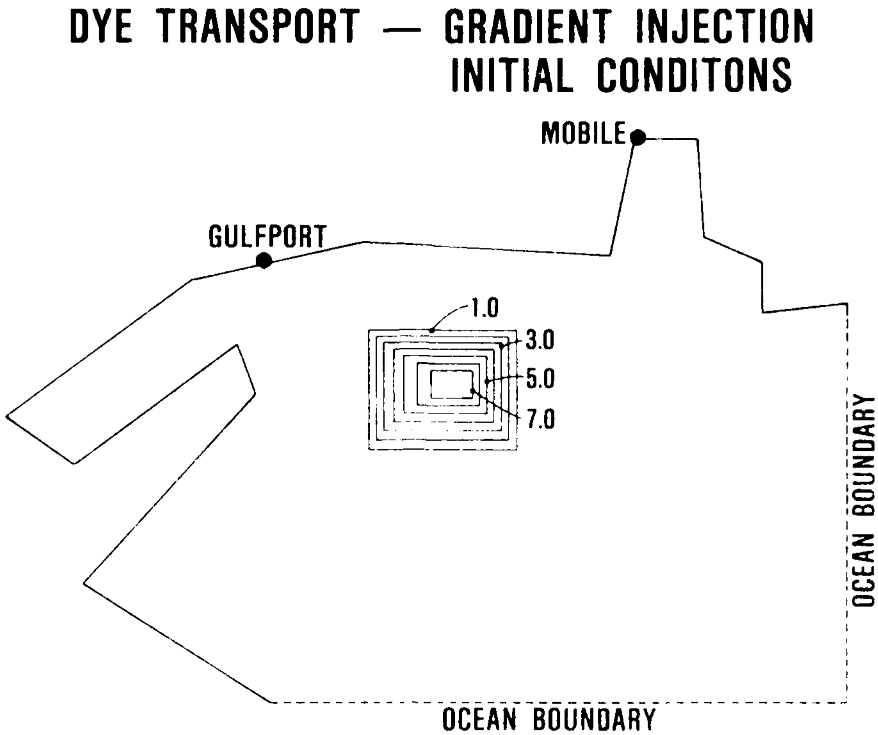

Figure 21. Mississippi Sound, WASP gradient injection initial condition

spike injection are shown in Figure 22a. WASP results for this injection using a 6-hr time-step are shown in Figure 22b. Clearly, the WASP simulation is overdispersive in comparison with the WIFM-SAL results. Unlike the CE-QUAL-W2 solution scheme (i.e., unlike CE-QUAL-W2, WIFM-SAL is not inherently overdispersive), the flux-corrected transport scheme in WIFM-SAL controls numerical dispersion. The spike injection into the Mobile Bay area, using a direct box model overlay on the WIFM-SAL grid, illustrates that for a one-to-one grid overlay, the box model is overdiffusive in comparison with WIFM-SAL transport. Figure 23 demonstrates this using time-steps as long as 6 and 12 hr for the box model simulation. Peak concentrations for the box model simulation are twofold to threefold lower than peak values maintained by WIFM-SAL.

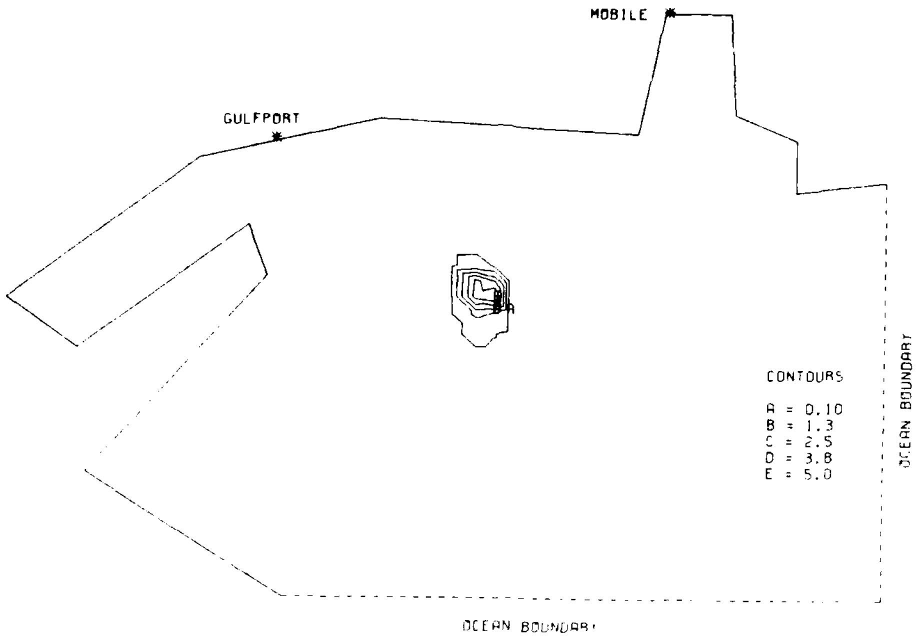

a. WIFM-SAL results

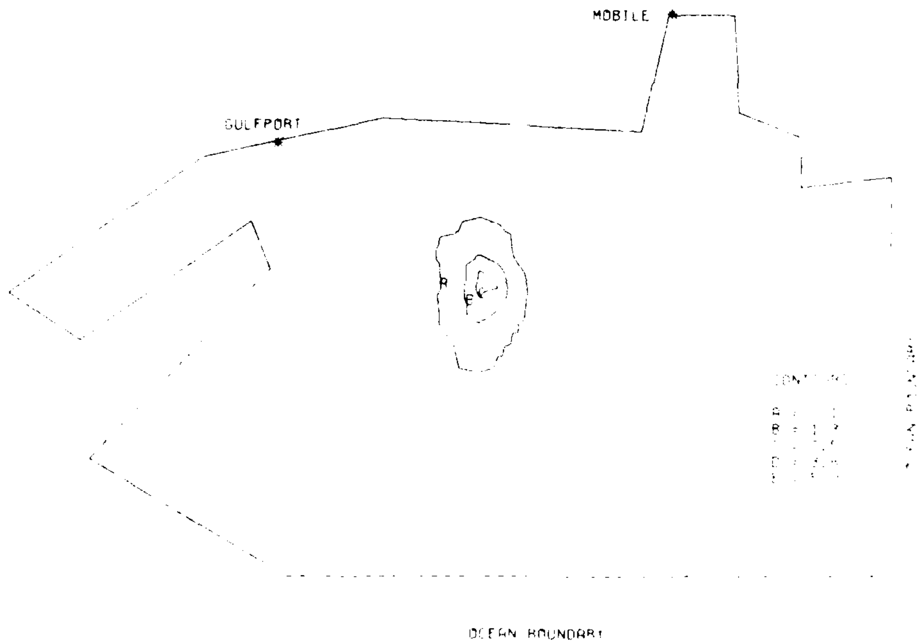

b. Box model results for 1:6 overlay

Figure 22. Mississippi Sound, concentration contours after 4.5-day simulation for instantaneous injection in WASP segment 683

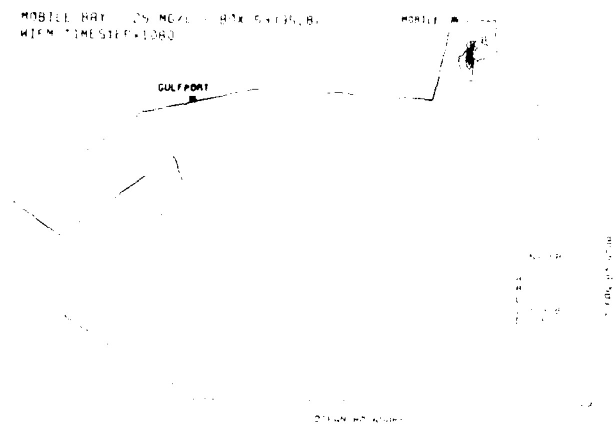

a. WIFM-SAL results

b. Box model results using 1:1 overlay and 6.0-hr time-step

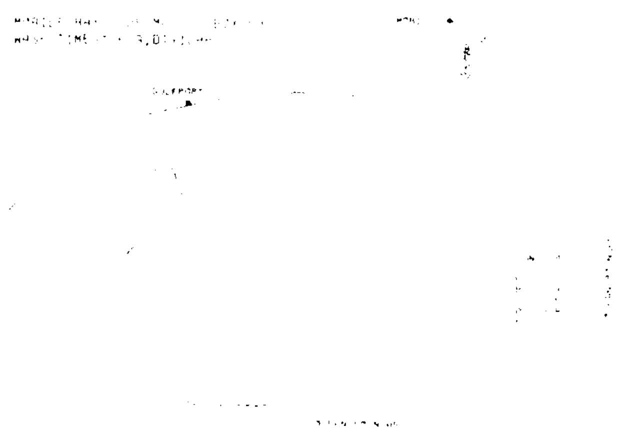

c. Box model results using 1:1 overlay and 12.0-hr time-step

Figure 23. Mobile Bay instantaneous injection after 4.5-day simulation

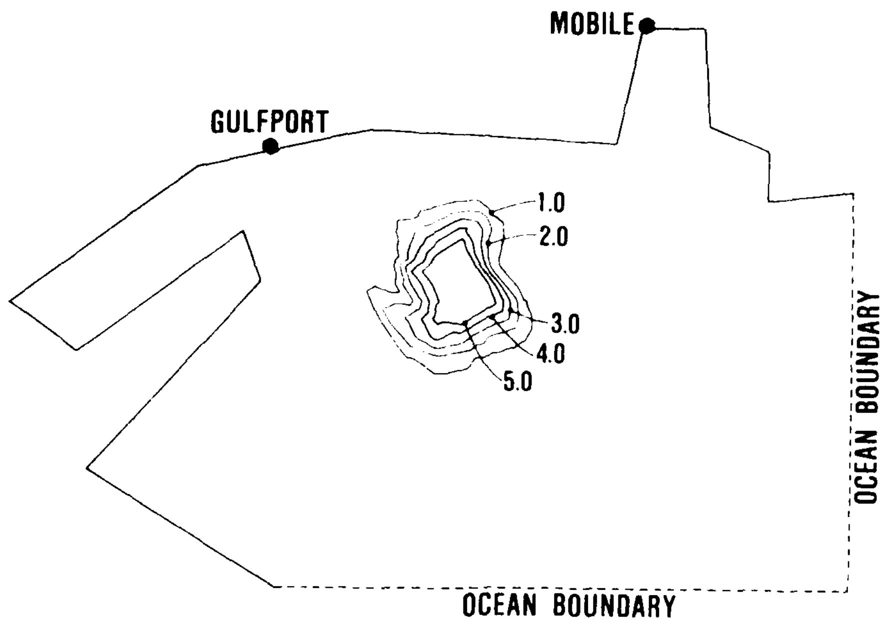

a. WIFM-SAL

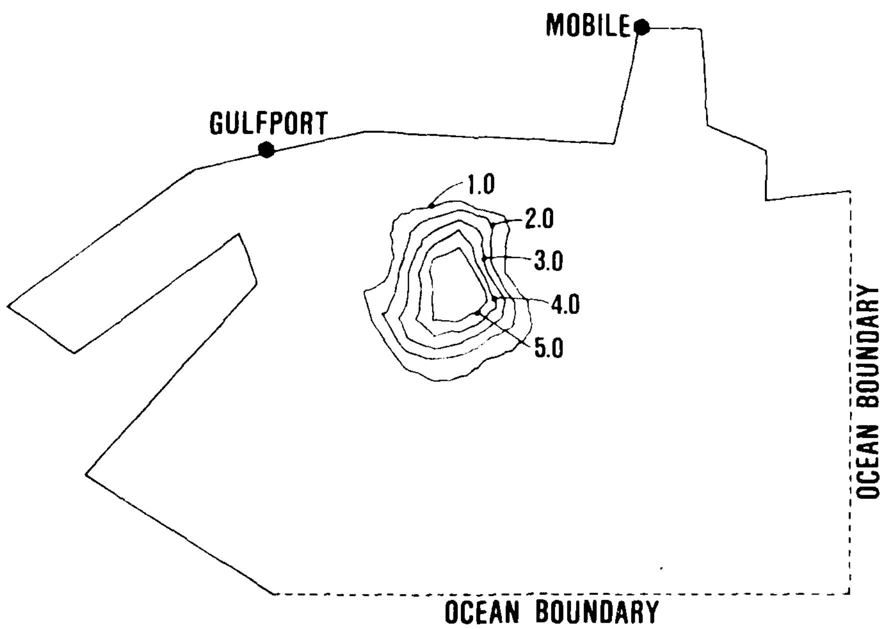

b. 6:1 Model simulation

Figure 24. Mississippi Sound, results of gradient injection after 4.5-day simulation

41. For most water quality considerations, a gradient of the constituents rather than a sharp front exists. For the 6:1 overlay 6-hr time-step and the initial conditions described in Table 4, results are shown in Figure 24. Although the overdispersive character of the box model is still discernible, the box model more closely replicates the transport for the gradient injection condition than for the steep front condition.

PART V: SUMMARY AND RECOMMENDATIONS

42. The box model is a computationally feasible approach for long-term multidimensional water quality modeling. For the applications described in this report, the box model required under 15-min CPU time, whereas the simulations using the directly linked models, CE-QUAL-W2 and WIFM-SAL, required from 3.0- to 20.0-hr VAX 11/750 CPU time. Computational time requirement is an important consideration for a complex water quality application requiring a large number of calibration runs and long-term (seasonal and annual) simulations.

43. The box model is numerically diffusive. An increase in box model segment size increases numerical diffusion. Numerical diffusion decreases as the time-step increases until numerical instabilities occur; i.e., as the Courant number approaches one, numerical diffusion approaches zero.

44. Box model simulation results compare well with results obtained using CE-QUAL-W2. Using a one-to-one grid overlay, box model results are nearly identical to CE-QUAL-W2 results. The upwind difference scheme in CE-QUAL-W2 is also a diffusive scheme and is equivalent to the box model solution. However, even using a one-to-one grid overlay and time-steps up to 12 hr, the box model is overdiffusive in contrast to WIFM-SAL, which has a diffusion-controlled solution.

45. Neither the box model nor CE-QUAL-W2 is appropriate for simulating a situation where movements of sharp fronts of material, such as spills, must be depicted accurately. Both are, at present, numerically overdiffusive; i.e. numerical diffusion at the model in many instances exceeds physical diffusion in the system. However, for situations where concentration gradients are not steep, these models can adequately represent the mass transport in a water body. This limitation is acceptable for many water quality applications. At the time of this publication, both models were being modified to reduce numerical diffusion.

46. Extensive effort to accurately determine the mass dispersion coefficients for a multidimensional modeling study, using either the box model or CE-QUAL-W2 with its current transport algorithm, appears to be unnecessary, since numerical diffusion in these models is typically greater than the physical dispersion for the system. However, where intertidal averaging is

performed, additional dispersion may need to be input, and calculation of this parameter could be crucial.

47. Future activities should focus in the following three areas:

   a. Linkage of the box model with other hydrodynamic models including CELC3D, a three-dimensional stretched grid model; CH2D, the two-dimensional boundary-fitted hydrodynamic model; and CH3D, the three-dimensional boundary-fitted hydrodynamic model.

   b. Integration of a diffusion-controlled solution scheme in the box model and CE-QUAL-W2 (see paragraph 45).

   c. Testing of the use of intertidally averaged hydrodynamics with the box model and development of methods to calculate advective flows and dispersion coefficients for the box model for these intertidal cases from the hydrodynamic model output.

REFERENCES

Crank, J. 1984. The Mathematics of Diffusion, Clarendon Press, Oxford.

Ditoro, D. M., Fitzpatrick, J. J., and Thomann, R. V. 1983. "Documentation for Water Quality Analysis Simulation Program (WASP) and Model Verification Program (MVP)," EPA-600/3-81-044, Washington, DC.

Edinger, J. E., and Buchak, E. M. 1981. "Estuarine Laterally Averaged Numerical Dynamics: The Development and Testing of Estuarine Boundary Conditions in the LARM Code," Miscellaneous Paper EL-81-9, prepared by J. E. Edinger Associates, Inc., for the US Army Engineer Waterways Experiment Station, Vicksburg, Miss.

Environmental Laboratory (EL). 1986. "CE-QUAL-R1: A Numerical One-Dimensional Model of Reservoir Water Quality; User's Manual," Instruction Report E-82-1 (Revised Edition), US Army Engineer Waterways Experiment Station, Vicksburg, Miss.

__________. "A Dynamic One-Dimensional (Longitudinal) Water Quality Model for Streams, CE-QUAL-RIV1: User's Manual," Instruction Report in preparation, US Army Engineer Waterways Experiment Station, Vicksburg, Miss.

Environmental and Hydraulics Laboratories. 1986. "CE-QUAL-W2: A Numerical Two-Dimensional, Laterally Averaged Model of Hydrodynamics and Water Quality: User's Manual," Instruction Report E-86-5, US Army Engineer Waterways Experiment Station, Vicksburg, Miss.

Fischer, H. B. 1976. "Mixing and Dispersion in Estuaries," Annual Review of Fluid Mechanics 8, pp 107-133.

Fischer, H. B., et al. 1979. Mixing in Inland and Coastal Waters, Academic Press, Inc., New York.

Hall, R. W. 1987. "Application of CE-QUAL-W2 to the Savannah River Estuary," Technical Report EL-87- , US Army Engineer Waterways Experiment Station, Vicksburg, Miss.

Kuo, J. T., and Thomann, R. V. 1984. "Phytoplankton Modeling in the Embayments of Lakes," Journal of Environmental Engineering, Vol 109, No 6.

Martin, J. L. 1987. "Application of a Two-Dimensional Model of Hydrodynamics and Water Quality (CE-QUAL-W2) to DeGray Lake, Arkansas," Technical Report E-87-1, US Army Engineer Waterways Experiment Station, Vicksburg, Miss.

Roache, Patrick J. 1982. "Computational Fluid Dynamics," Hermosa Publishers, Albuquerque, N. Mex.

Schmalz, Richard A., Jr. 1985a. Numerical Model Investigation of Mississippi Sound and Adjacent Areas, Miscellaneous Paper CERC-85-2, US Army Engineer Waterways Experiment Station, Vicksburg, Miss.

__________. 1985b. User Guide for WIFM-SAL: A Two-Dimensional Vertically Integrated, Time-Varying Estuarine Transport Model, Instruction Report EL-85-1, US Army Engineer Waterways Experiment Station, Vicksburg, Miss.

Shanahan, P., and Harleman, D. R. F. 1984. "Transport in Lake Water Quality Modeling," Journal of Environmental Engineering, Vol 110, No. 1.

ATE

LMED

8